

A Ped's Story: Weathering Out Climatic Change During the mid-Cretaceous

Aisha H. Al-Suwaidi
B.ES. The University of Arizona, 2004

Submitted to the Department of Geology and the
Faculty of the Graduate School of the University of Kansas
In partial fulfillment
of the requirements for the degree
Master's of Science

Advisory Committee:

Luis A. González
(Chair)

Gregory A. Ludvigson
(Co-Chair)

Daniel F. Stockli

Date Defended _____

The Thesis committee for Aisha H. Al-Suwaidi certifies
That this is the approved version of the following thesis:

A Ped's Story: Weathering Out Climatic Change During the mid-Cretaceous

Advisory Committee:

**Luis A. González
(Chair)**

**Gregory A. Ludvigson
(Co-Chair)**

Daniel F. Stockli

Date Approved: _____

A Ped's Story: Weathering Out Climatic Change During the mid-Cretaceous

By

Aisha H. Al-Suwaidi

Abstract

The upper Ruby Ranch Member and basal Mussentuchit Member of the Cedar Mountain Formation in the vicinity of the Price River II Quarry (CEU-PR2) in the Price River area, East Central Utah, consists of fluvially derived sediments in a floodplain environment with a seasonal xeric regime. Bulk organic matter carbon isotope chemostratigraphic profiles $\delta^{13}\text{C}_{\text{org}}$ for measured sections in the CEU-PR2 area are constrained by detrital zircon ages ranging from 109 to 116 Ma (Burton et al., 2006). These $\delta^{13}\text{C}_{\text{org}}$ profiles show prominent excursions and structure that have been correlated with global $\delta^{13}\text{C}_{\text{org}}$ chemostratigraphy of Bralower et al. (1999) and show carbon excursion events C10-C13. This correlation suggesting that the Aptian-Albian boundary is captured by the Ruby Ranch Member and makes the upper most Ruby Ranch Member and Mussentuchit Member strictly Albian in age.

Acknowledgements

I would like to acknowledge, the College of Eastern Utah and The Utah Geological Survey, James Kirkland and Martha Hayden, for their support in the field. Graduate students and staff at the University of Kansas, who have helped and offered support along the way, in the field and lab including Greg Cane, the Suarii and graduate students at Isotope Geochemistry Lab.

Table of Content

	<i>Page</i>
Title Page	1
Acceptance Page	2
Abstract	3
Acknowledgements	4
Table of Contents	5
List of Figures	8
A Ped's Story: Weathering Out Climatic Change During the mid-Cretaceous	
I. Abstract	9
II. Introduction	10
1. Geologic Setting	13
2. Mid-Cretaceous Paleoclimate	16
3. Carbon Excursions and Ocean Anoxic Events	19
III. Methods	21
1. Field Collection	21
2. Sample Preparation and Analysis	22
IV. Results	22
1. Description of Stratigraphic Profiles	22
a. KU-PR1 Facies Description	22
b. KU-PR2 Facies Description	32

i. Lower-KU-PR2 Facies Description	33
ii. Upper-KU-PR2 Facies Description	42
c. KU-PR3/4 Facies Description	47
i. KU-PR4 Facies Description	47
ii. KU-PR3 Facies Description	51
2. Description of Chemostratigraphic Profiles	54
a. KU-PR1 chemostratigraphy	54
b. KU-PR2 chemostratigraphy	57
c. KU-PR3/4 chemostratigraphy	60
V. Discussion and Interpretation	63
1. Facies Distribution	63
a. Fluvial channel	63
b. Palustrine and Lacustrine, calcretes and sediments	65
c. Paleosol	66
2. Interpretations	67
a. Paleoenvironmental Interpretation	67
b. Chemostratigraphic Interpretation	67
VI. Conclusion	72
VII. References	76
Appendices	83
Appendix A. Field Notes KU-PR1	83
Appendix B. Field Notes KU-PR2	96

Appendix C.	Field Notes KU-PR3/4	105
Appendix D.	Stable isotope data KU-PR1	119
Appendix E.	Stable isotope data KU-PR2	121
Appendix F.	Stable isotope data KU-PR3/4	122
Appendix G.	Muddy Creek Section	124
Appendix H.	Geochronology and stable isotope data	
	KU-Muddy Creek	130

List of Figures

Figure 1. Map of Utah and Cedar Mountain Formation	11
Figure 2. A generalized column of Utah's Late Mesozoic strata	14
Figure 3. Paleogeography	17
Figure 4. Measured sections for KU-PR1, KU-PR2 and PR3/4	23
Figure 5. Composite image of section at KU-PR1	25
Figure 6. Composite image of KU-PR2-CU1	34
Figure 7. Composite images of KU-PR2-CU2A and B	37
Figure 8. KU-PR2-CU3 and KU-PR2-CU4	40
Figure 9. KU-PR2 upper section	43
Figure 10. KU-PR3/4 stratigraphic section	48
Figure 11. Chemostratigraphic profile of KU-PR1	55
Figure 12. Chemostratigraphic profile of KU-PR2	58
Figure 13. Chemostratigraphic profile of KU-PR3/4	61
Figure 14. Chemostratigraphic profiles showing $\delta^{13}\text{C}_{\text{org}}$ (‰)	70
Figure 15. Chemostratigraphic profile and stratigraphy	73

A Ped's Story: Weathering Out Climatic Change During the mid-Cretaceous

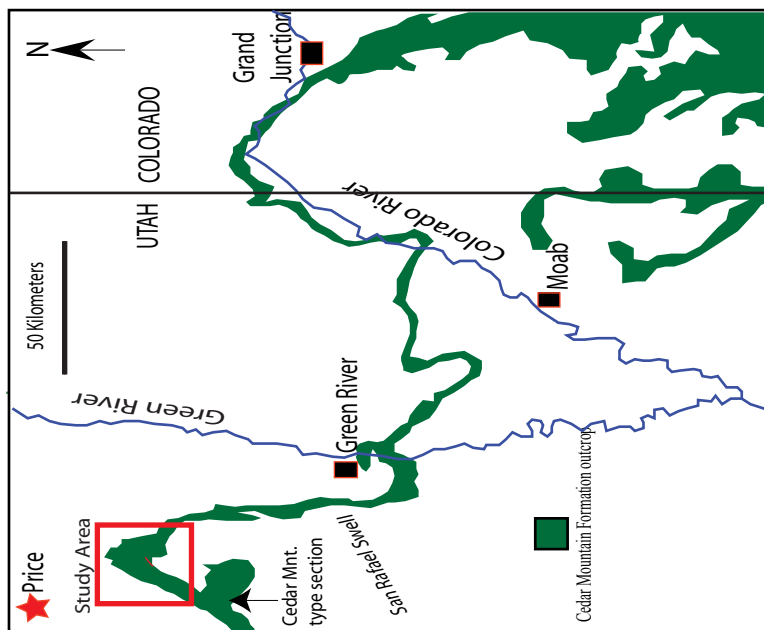
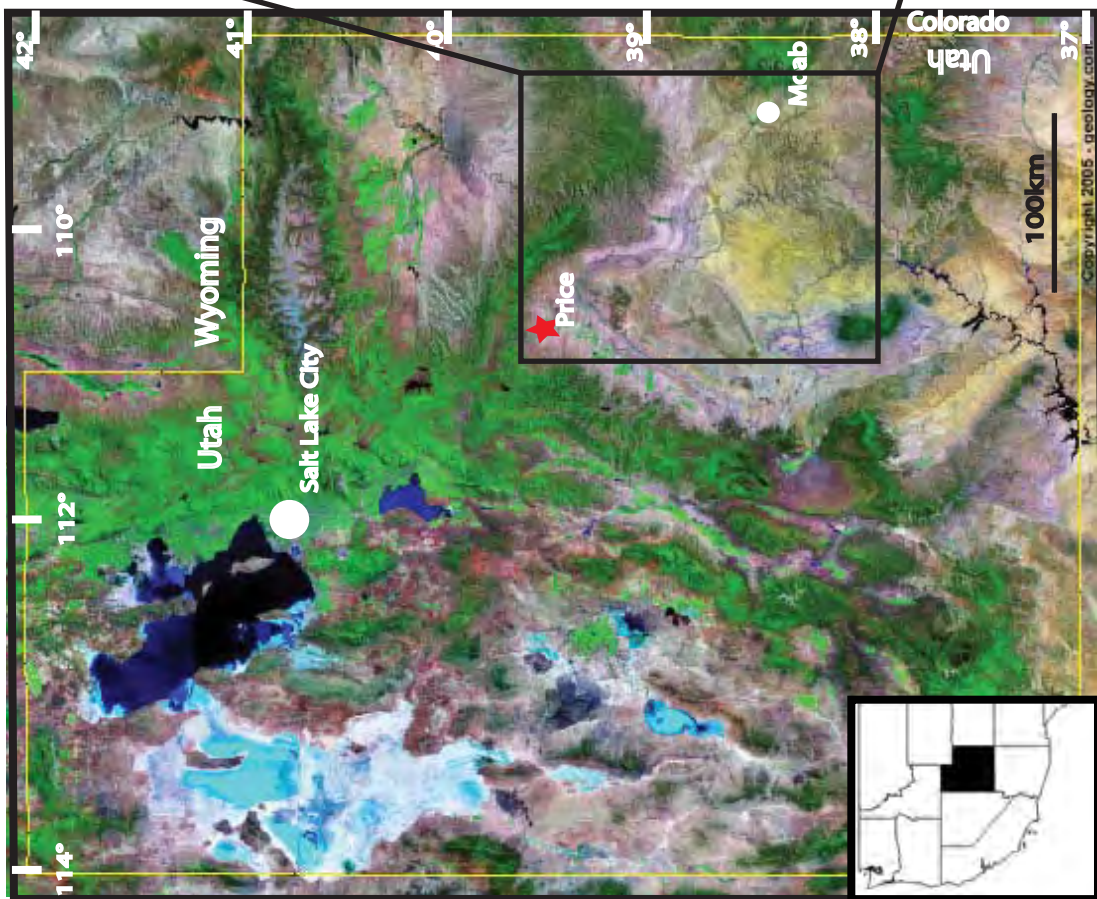
Abstract

The upper Ruby Ranch Member and basal Mussentuchit Member of the Cedar Mountain Formation in the vicinity of the Price River II Quarry (CEU-PR2) in the Price River area, East Central Utah, consists of fluvially derived sediments in a floodplain environment with a seasonal xeric regime. Bulk organic matter carbon isotope chemostratigraphic profiles $\delta^{13}\text{C}_{\text{org}}$ for measured sections in the CEU-PR2 area are constrained by detrital zircon ages ranging from 109 to 116 Ma (Burton et al., 2006). These $\delta^{13}\text{C}_{\text{org}}$ profiles show prominent excursions and structure that have been correlated with global $\delta^{13}\text{C}_{\text{org}}$ chemostratigraphy of Bralower et al. (1999) and show carbon excursion events C10-C13. This correlation suggesting that the Aptian-Albian boundary is captured by the Ruby Ranch Member and makes the upper most Ruby Ranch Member and Mussentuchit Member strictly Albian in age.

Introduction

Soils are imprinted through pedogenesis with a characteristic signal of the environmental conditions directly associated with the hydrology, ecology and climate of the region in which they form. The imprint can be analyzed in paleosols using sedimentologic, petrographic, and geochemical techniques to unravel the paleohydrology, paleoecology and paleoclimate of a region. The paleosols and sediments of the Aptian-Albian Cedar Mountain Formation (CMF), in east-central Utah (Fig. 1) provide an opportunity to examine sediments that underwent pedogenesis during one of the most recent extreme greenhouse periods. In comparison to the present, temperatures may have been 6-12°C warmer (Barron, 1995), and atmospheric CO₂ concentrations are estimated to have been 2 to 6 times higher (Barron et al., 1993; Cerling, 1991; Poulsen et al., 2001). Moreover other greenhouse gases (e.g. H₂O_v and CH₄) could have been much higher than at present (Barron et al., 1995a; Barron et al., 1993). Recent studies show an intensification of the hydrologic cycle in North America during the late Albian (Ufnar et al., 2002; White et al., 2001). The mid-Cretaceous (Aptian-Cenomanian) also had multiple ocean anoxic events (OAE's) (Leckie et al., 2002; Poulsen et al., 2001) and methane hydrate releases (Jahren et al., 2001; Larson and Erba, 1999), which had drastic but short-lived impacts on the atmosphere, biosphere and pedosphere. This was also a period of major origination and diversification of angiosperms (Heimhofer et al., 2005) and dinosaurs (Serenó, 1997), of which there are many remains and traces preserved in the CMF (Fig. 2) (Kirkland, 2005; Lockley et al., 2004).

Figure 1. Map of Utah, showing the relative location of the of the study area (King, 2005; <http://geology.com/satellite/utah-satellite-image-m.jpg>). The Cedar Mountain type section and distribution of the Cedar Mountain Formation in Eastern Utah are also shown (Adapted from Kirkland et al. 2005).



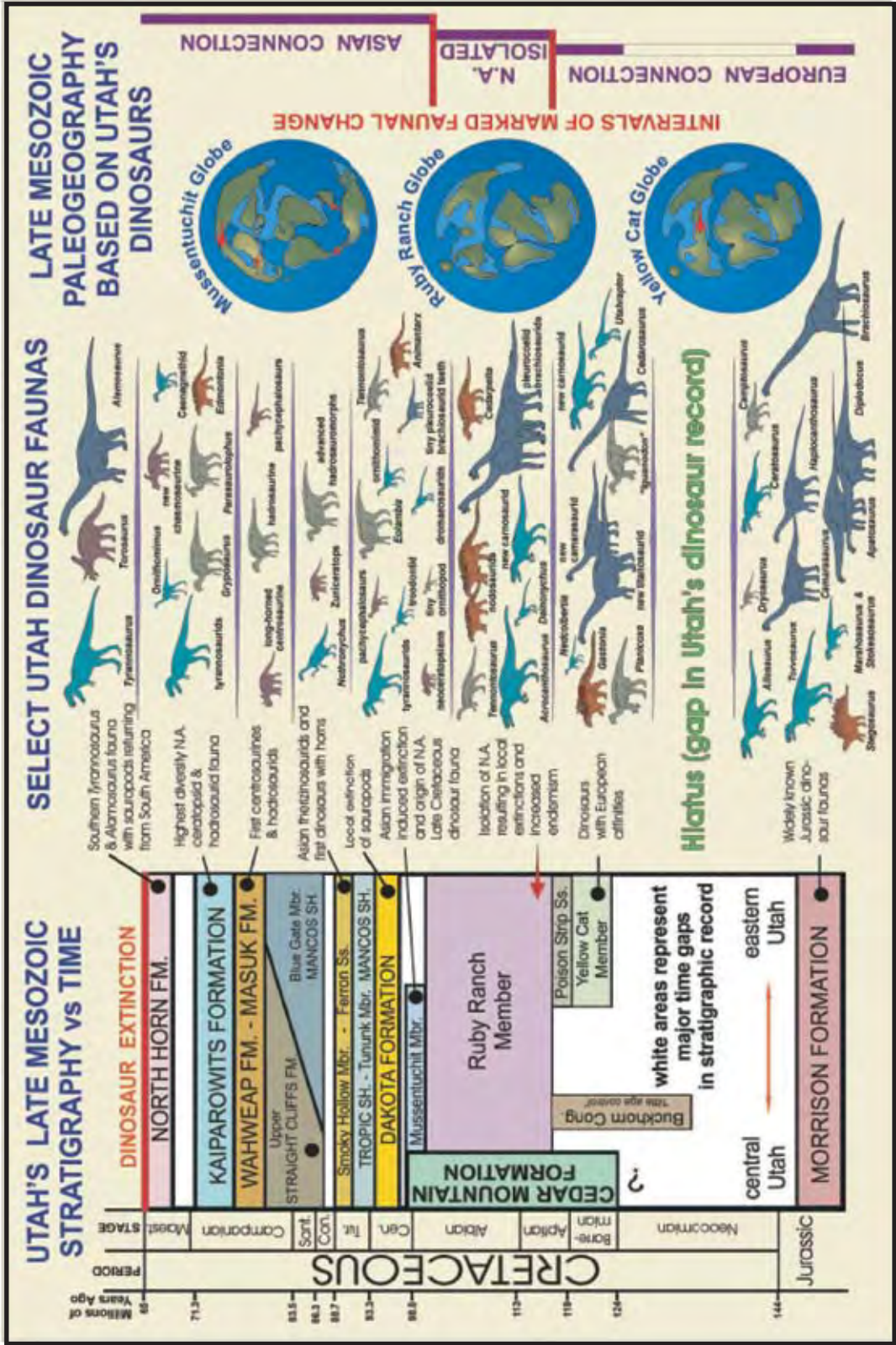
This study examines the Ruby Ranch and Mussentuchit Members of the Cedar Mountain Formation in the vicinity of the College of Eastern Utah, Price River II dinosaur quarry (CEU-PR2) in the North Western San Rafael Swell, Carbon County, Utah (Fig. 1). CMF paleosols and sediments, and carbonate rocks were analyzed for their stable organic carbon ($\delta^{13}\text{C}$) isotopes to generate a record of environmental change during the Aptian-Albian. This record will allow us to better understand and possibly quantify the paleohydrologic and paleoclimatic changes taking place during the Aptian-Albian. Understanding and quantification of the mid-Cretaceous greenhouse world will aid in understanding the response of terrestrial ecosystems to ongoing global warming. Because present atmospheric CO_2 concentrations exceed those estimated for the Pleistocene (Brook, 2005; Petit et al., 1999) the mid-Cretaceous is possibly our best analogue for future CO_2 -induced warming.

Geologic setting

The Cedar Mountain Formation (CMF) comprises five units, the Buckhorn Conglomerate, the Yellow Cat Member, the Poison Strip Sandstone, the Ruby Ranch Member, and Mussentuchit Member (Kirkland et al., 1999; Sprinkel et al., 1999; Stokes, 1952) (Fig. 2).

The Yellow Cat Member and Poison Strip sandstone crop out on the East side of the San Rafael Swell and are not present in the study area. Instead the Buckhorn Conglomerate unconformably overlies the Upper Jurassic (Tithonian) Morrison Formation in the area of study. It is overlain by the Upper Cretaceous (Cenomanian) Dakota Formation (Fig.2). The Ruby Ranch and Mussentuchit Members of the CMF

Figure 2. A generalized column of Utah's Late Mesozoic strata plotted against the geological time scale with a summary of Utah's preserved dinosaur faunas and resulting continental paleogeographic patterns these dinosaurs indicate (Kirkland et al., 2005).



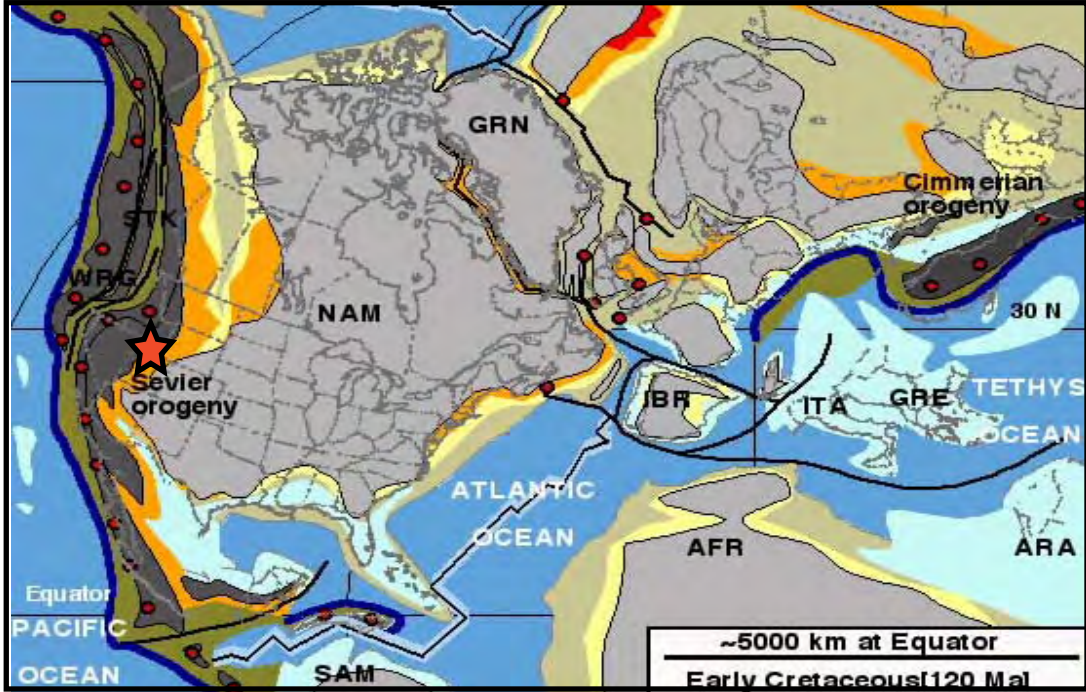
are considered to be Aptian-Albian in age based on single crystal U/Pb ages of detrital zircons (Burton et al., 2006) and $^{40}\text{Ar}/^{39}\text{Ar}$, sanidine crystal ages from primary ash falls (Cifelli et al., 1997; Garrison et al., 2007) as well as (U-Th)/He and Pb-Pb ages from single detrital zircon crystals conducted at the The University of Kansas Isotope Geochemistry Lab (Appendix H).

During the mid-Cretaceous, the ancestral Rockies and Sevier Mountain Ranges to the West, and the Western Interior Sea way to the East would have flanked this area (Fig. 3). The siliciclastic detritus contained in the units of the CMF were derived from the Sevier Mountains and deposited in the fore bulge deposition zone of the associated foreland basin (Currie, 2002; Yingling and Heller, 1992). These sediments underwent episodic pedogenesis, and accumulated in fluvial, lacustrine, and palustrine environments (Currie, 2002; Nelson and Crooks, 1987; Sprinkel et al., 1999). Significant work has been done to try to understand the provenance of sediments in the Jurassic-Cretaceous cordilleran foreland basin associated with the Sevier thrust belt. But constraints on timing of thrust and flexural events that created sediment accommodation in the lower Cretaceous interval are limited. (Currie, 1998, 2002; DeCelles, 2004; DeCelles and Currie, 1996; Yingling and Heller, 1992)

Mid-Cretaceous Paleoclimate

During the Aptian-Albian, climate in east-central Utah was seasonally wet with a long lasting dry season (Kirkland et al., 1999) resulting in a savannah-like environment and seasonal precipitation that sustained fluvial systems and lakes

Figure 3. Paleogeography, including major orogenic belts, and other geographic artifacts. Red star indicates approximate location of study area, in the vicinity of Price River, near the College of Eastern, Utah PR-2 dinosaur quarry (Utah Geological Survey accession # Em372). The site location information for CEU-PR2 is held in confidential status by the office of the Utah State Paleontologist at the Utah Geological Survey (contact information in Appendix A). (Blakey, 2001; http://jan.ucc.nau.edu/~rcb7/Early_Cretaceous.html).



Key:

List of Visible Plates & Abbreviations:

AFR= Africa	IBR= Iberia (Spain & Portugal)
ARA= Arabia	ITA= Italy
GRE= Greece	NAM= North America
GRN= Greenland	SAM= South America

(Hallam, 1985, 1986). The Sevier orogenic belt also had an orographic effect on climate (Fig.3). The change in abundance of calcareous horizons has led researchers to conclude that climate became wetter from the time of formation of the Ruby Ranch member to the Mussentuchit member (Cifelli et al., 1999; Kirkland et al., 1999).

The Cretaceous is considered to be one of the warmest global greenhouse periods in recent geological history (Spicer and Corfield, 1992). With elevated carbon dioxide, and other greenhouse gasses (including methane and water vapor) the mid-Cretaceous greenhouse maximum is thought to have had temperatures from 6°-14°C warmer than present and atmospheric carbon dioxide 4-6 times higher than present (Barron et al., 1995b). Plant and faunal fossil records from very high latitudes provide us with evidence of an ice free Arctic, with fossil evidence of extensive deciduous forests at about 75°-85°N (Spicer and Corfield, 1992). Sea levels are estimated to have been about 20m higher than present (Poulsen et al., 2001) with sea surface temperatures in the mid-Cretaceous as high as 31°-33°C in the low latitudes and 16°C warmer than present in the high latitudes (Barron et al., 1995b). The continents were clustered mostly at the mid-low latitudes (Spicer and Corfield, 1992).

Carbon Isotope Excursions and Ocean Anoxic Events

Ocean Anoxic Events are periods of elevated marine organic carbon burial that led to a drawdown in atmospheric carbon dioxide, and depletion of oceanic oxygen leading to ocean anoxia and dysoxia, and are events of extensive black shale

deposition (Erbacher et al., 2001; Jenkyns, 1980). Cretaceous OAE's are related to major perturbations in global oceanic circulation and are temporally associated with the onset of pronounced carbon isotope excursions ($\geq 1.5\%$) both leading and following OAE's (Bralower et al., 1999; Grocke et al., 1999; Jenkyns, 2000; Jenkyns, 2003).

There are many mechanisms that could have resulted in these carbon isotope excursions and the associated OAE's including; high rates of sea floor spreading and off ridge volcanism, which were higher during this period than any other time (Bralower et al., 1999; Poulsen et al., 2001) and may have led to carbon isotope excursions as isotopically lighter carbon dioxide was released to the atmosphere. Other researcher's have suggested that the thermal disassociation of methane hydrates in deep oceans could have led to the release of isotopically lighter carbon (Jahren et al., 2001). Other suggested causes for OAE's include, the warming of ocean bottom water, destratifying and limiting oxygen availability throughout the water column. Increased input of continental organic matter into the water column due to increased land runoff and high vegetation productivity on land, would have led to increased nutrient availability resulting in increase plankton productivity, that could have through time created anoxic conditions as excess planktonic biomass decomposed in the water column (Leckie et al., 2002).

Methods

Field Collection

Fieldwork was conducted for four weeks in July 2005 and a week in June 2006. The strata overlying and underlying College of Eastern Utah, Price River dinosaur quarry number 2 (CEU-PR2; Utah Geological Survey accession number Em372) were the major focus of this study and two additional sites were selected from the surrounding vicinity. Site information is held in confidential status by the office of the Utah State Paleontologist at the Utah Geological Survey, contact information maybe found in Appendix A. One stratigraphic section was measured and described at each of these sites, KU-PR1, KU-PR2, and KU-PR3. Site KU-PR1 is approximately 2 km North West of CEU-PR2 and is located near Price River. KU-PR2 corresponds to CEU-PR2 site. The third site, KU-PR3 is approximately 0.50 km South East of CEU-PR2. These sites also had expression of a major carbonate unit that appeared to be locally extensive and similar to the one present at CEU-PR2.

Stratigraphic sections were measured and described along trenched surfaces. Oriented samples were collected at 1m intervals, however most carbonate beds were sampled at 50 cm interval or higher resolutions. Samples were also collected at boundaries where any lithologic or significant color change occurred. At these intervals, color, lithology, sedimentary structures as well as the presence of any fossils or trace fossils were noted.

Sample Preparation and Analysis

All sample analyses were conducted at the University of Kansas W. M. Keck Paleoenvironmental and Environmental Stable Isotope Laboratory under the direction of L. Gonzalez.

Samples for organic $\delta^{13}\text{C}$ were sampled from unpolished samples, using 1mm carbide drill milling bits. A gram of powdered sample was collected and then decarbonated using a procedure modified after that of Midwood and Boutton (1998). Samples were dried for 24-48 hours at 60°C to constant weight. Samples were decarbonated with 30 mL of 0.1 M hydrochloric acid (HCL) for 24 hours, rinsed and dried again to constant weight. These samples were weighed into silver capsules and combusted at 1060°C using a Costech Elemental Analyzer connected via a CONFLO III to the inlet of a ThermoFinnigan MAT 253 isotope ratio mass spectrometer. Instrument precision was monitored through daily analysis of three reference materials (DORM-2, USGS-24 and ANU-Sucrose). All isotope data are reported using δ notation relative to V-PDB.

Results

Stratigraphic Sections

Price River 1 (KU-PR1), near Price River

The Price River 1 section site was chosen largely due to the extensive exposure of Ruby Ranch and Mussentuchit members at this locality. The section is located approximately 12 km southeast of Wellington, Utah along the North bank of

Figure 4. Measured sections for KU-PR1 to PR3/4 correlated at the gradational boundary between Mussentuchit and Ruby Ranch Member's of the Cedar Mountain Formation, based on lithological change and biostratigraphy. Color variation in the between lithologic units indicates the relative color of rocks. Figure also shows the approximate location of major carbonate units, described in the text (e.g. KU-PRx-CUx).

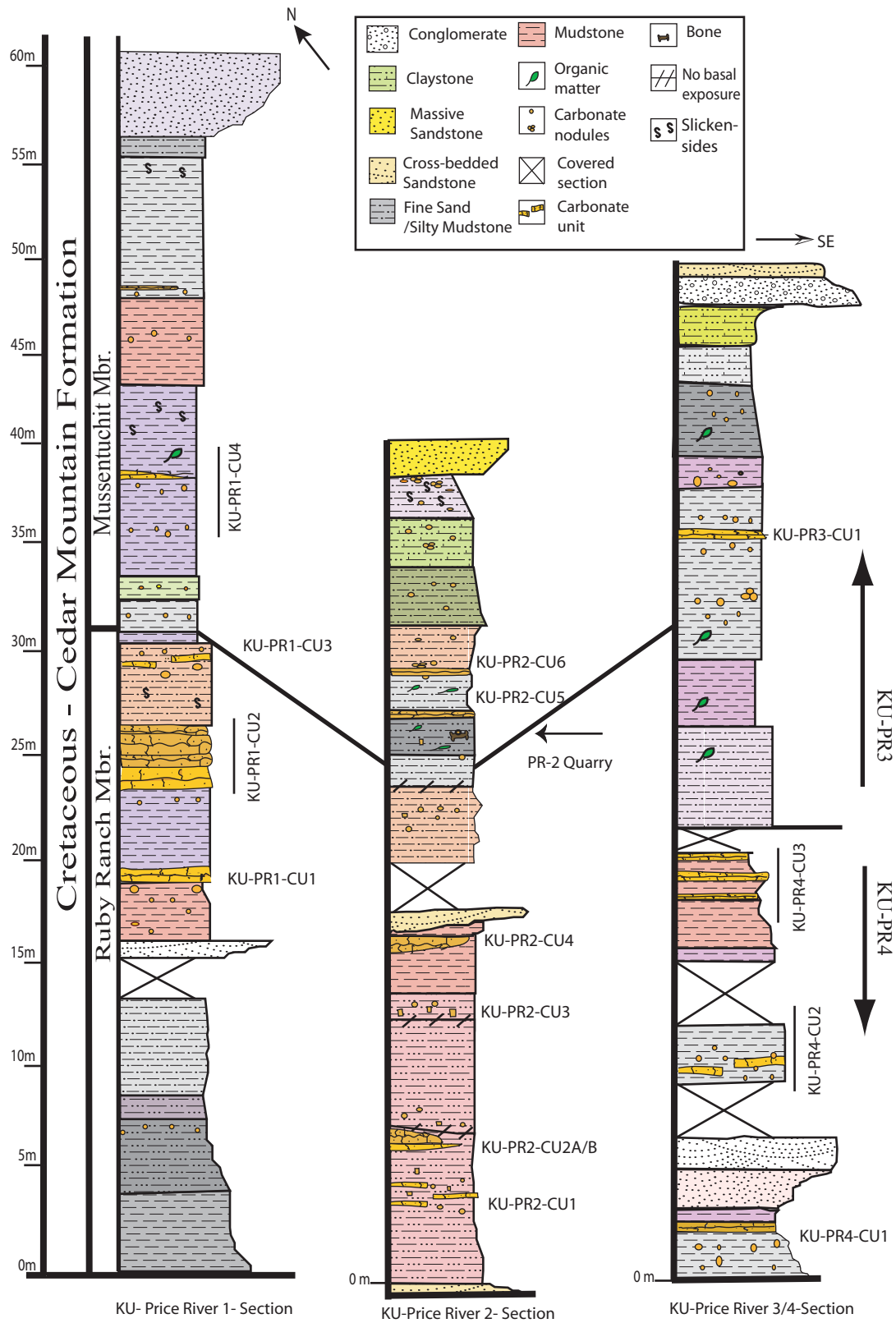
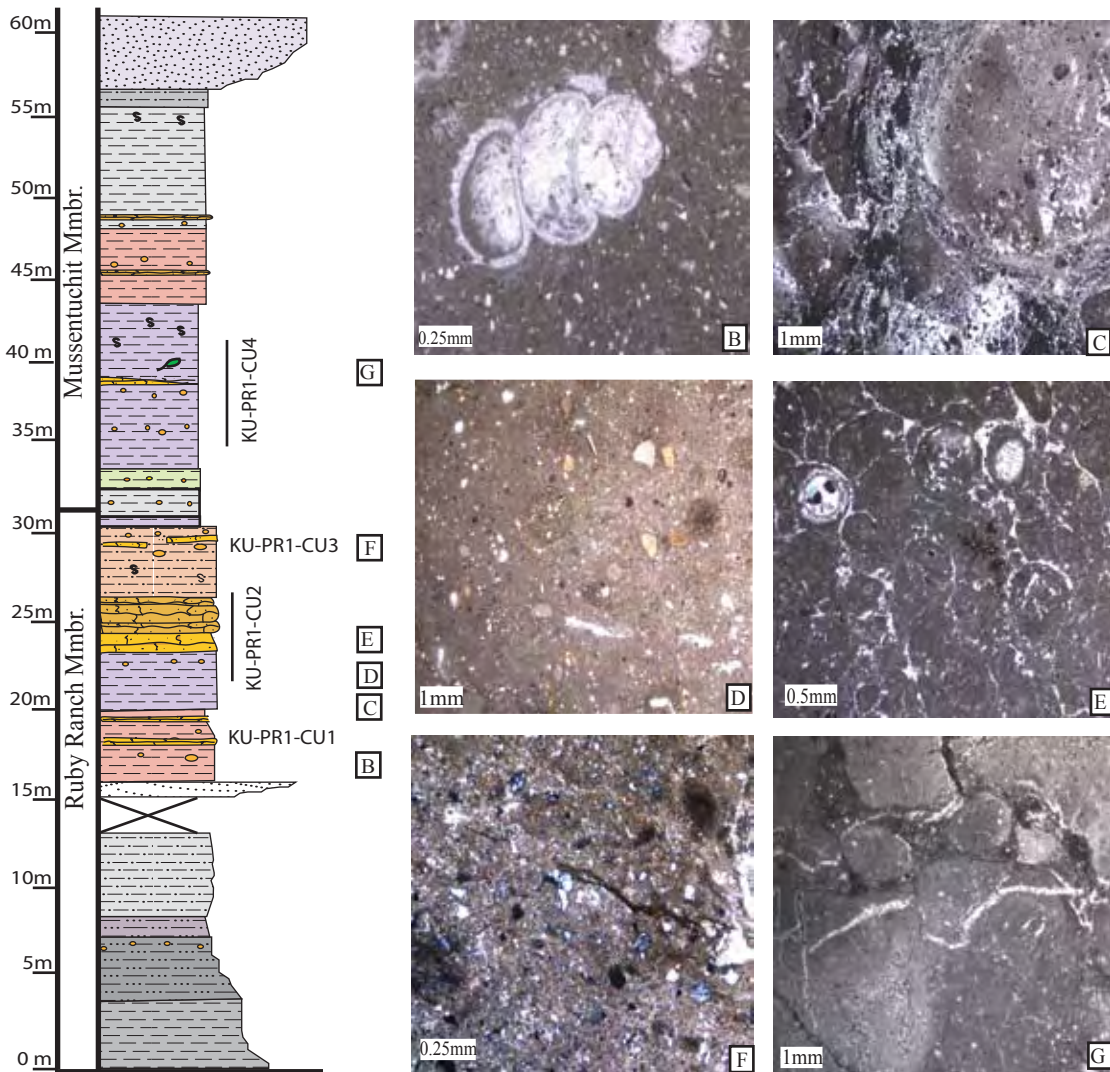


Figure 5. (A) Composite image of section at KU-PR1, showing boundary between Ruby Ranch and the Mussentuchit Member of the Cedar Mountain formation. Approximate location of thin sections and carbonate units described in the text (e.g. KU-PR1-CUx) is shown on the stratigraphic section. (B) Thin section showing gastropod in muddy matrix in plane light. Sparry calcite fill can be seen in the chambers of the shell. (C) Thin section showing micrite cemented mudstone, in cross polars. (D) Thin section of silty mudstone showing spar filled voids. (E) Cross-polarized thin section, showing charophytes, in a micritic matrix. (F) Cross-polarized thin section showing pelloidal mud with charophytes. (G) Thin section of mudstone, showing sparry calcite filled fractures and clotted mudstone matrix.



the Price River. It measures approximately 58 meters and extends through the Ruby Ranch member into the lowermost Mussentuchit member (Fig. 5A).

The section contains four interspersed indurated carbonate and carbonate nodule-bearing units. These carbonate units will be referred to as KU-PR1-CU1 to KU-PR1-CU4. KU-PR1-CU1 being the lowermost and KU-PR1-CU4 being the upper most carbonate unit. The base of the section is approximately 10 m above the Price River flood plain.

The lowermost unit is a dark gray massive mudstone measuring approximately 7.7 m, with macroscopic evidence of bioturbation and coalified organic matter. The clay content of this mudrock increases gradually toward the top of the unit. A ~1.2 m gradual color change from gray, to dark gray occurs at ~4.3 m. A purple mudstone at 8.6 m separates the overlying 6 m thick massive clay rich mudstone. The transition zone has scattered 0.1 to 1 cm diameter carbonate nodules. The uppermost mudstone is purple at the base and becomes greyer and less clay rich toward the top. It is highly weathered throughout with modern roots penetrating nearly all 6 meters.

At 13.4 m approximately 1.4 m of colluvium covers most of the transition from the weathered gray mudstone to the overlying sandstone. This sandstone interval from 15.3 m to 16.2 m, is cream colored cross-bedded, fining upward medium to coarse-grained sandstone. At the base of the sandstone 1 to 2 cm of mud are visible and suggest an unconformable (erosional?) contact. A purple-red

carbonate nodule bearing mudstone, KU-PR1-CU1 unconformably overlies this sandstone.

The KU-PR1-CU1 in the interval 16.3 m to 19.7 m is a massive carbonate nodule bearing calcareous purple-red mudstone with two 0.3 m carbonate indurated horizons at 18.2 m and 19.4 m respectively. The nodules range in diameter from 1 to 20 cm. At the base of the unit (16.2 m) carbonate nodules make up nearly 10% of the unit and over 1.6 m increase to almost 100%, forming a welded 0.3 m carbonate horizon. Immediately above the first indurated horizon (17.9 m above the base) carbonate nodules decrease to 10%, and gradually increase to nearly 100% over the next 1.2 m (19.4 m above the base), forming the second 0.3 m bed of indurated carbonate. Thin section examination of mudrock and nodules reveals burrows in a bioturbated micritic mudstone and well-preserved charophytes, gastropods, and ostracodes (Fig. 5B).

An abrupt contact at 19.7 m separates KU-PR1-CU1 from the overlying 2 m of massive featureless purple mudstone. The purple mudstone is slightly calcareous in the lower 0.2 m, but becomes non-calcareous and more clay rich gradually toward the top. At 22.5 m this purple mudstone transitions over a short distance into a dark purple calcareous mudstone that is 1.3 m thick. Carbonate nodules ranging from 1 to 10 cm in diameter occur in the upper 0.6 m of the mudstone (22.5 m to 23.1 m). Petrographic examination of the mudstone reveals micrite-cemented pelleted and clotted mud with burrowing and bioturbation (Fig. 5C, D).

The carbonate nodules in the upper 0.7 m increase gradually from approximately 5% to 100% abruptly transitioning at 23.1 m in to a welded, 3.6 m, massive featureless indurated orange carbonate bed, KU-PR1-CU2 (interval 23.1 m to 26.8 m). Petrographic examination of KU-PR1-CU2 reveals micrite-cemented clotted textured mudstone, with well-preserved charophytes, fish bioclasts, ostracodes, pellets, burrows and bioturbation (Fig 5E).

A sharp boundary at 26.8 m separates KU-PR1-CU2 from the overlying unit. The unit is a 2.8 m thick massive red mudstone with macroscopic slickensides and clay skins, and has highly variable amounts of calcium carbonate. However, calcium carbonate content is highest near the bottom (27.2 m) and top (28.7 m) of the unit and the central 1.0 m is non calcareous.

As the calcium carbonate content increases in the upper 1m of the red mudstone unit carbonate nodules are found scattered through the mudstone. The size of nodules increases toward the top from as small as 1 cm in diameter at the base to as large as 20 cm at the top. The abundance of carbonate nodules also increases from 5 % at the base to 25% at the very top of the mudstone. Petrographic examination reveals nodules to consist of micrite, the mudstone matrix is micrite-cemented and bioturbated. Microscopic rootlets, some surrounded by calcite microspar, and spar filled voids less than 0.25 mm in diameter are common in the mudstone matrix and carbonate nodule (Fig. 5F). A late chalcedony is observed in some voids.

The carbonate nodule bearing mudstone sharply transitions at 29.5 m to approximately 0.6 m of calcareous massive red mottled grey laminated mudstone. It

has macroscopic coalified organic matter and dark grey rip up clasts. The mudstone gradually transitions into KU-PR1-CU3 at 30.1 m.

KU-PR1-CU3, measures approximately 0.7 m in the interval 30.1 m to 30.8 m and grades from a carbonate nodule bearing massive red mudstone at 30.3 m, to a red mudstone interfingering with lenticular indurated carbonates at 30.5 m. The abundance and size of carbonate nodules increases rapidly from approximately 5% in the lower 0.2 m to about 25% in the upper 0.5 m, eventually forming the coalesced lenticular, indurated carbonate horizon. Nodules range in diameter from 5 to 20 cm, and increase in abundance towards the lenticular bed but are generally scattered through out KU-PR1-CU3.

The contact between KU-PR1-CU3 and the overlying unit at 30.8 m is sharp and most likely unconformable. The unit is a massive grey calcareous silty mudstone with dark grey mottles. The silty grey mudstone is approximately 2 m thick and contains scattered 0.1 to 3 cm diameter carbonate nodules. This mudstone appears to mark the beginning of the transition from the Ruby Ranch member to the more smectitic and gleyed Mussentuchit member at KU-PR1.

The silty grey mudstone gradually transitions to a non-calcareous green massive smectitic mudstone at ~32.7 m. This green smectitic mudstone is 0.7 m thick and contains small 1 to 2 cm diameter carbonate nodules in the upper 0.2 m. The non-calcareous mudstone is overlain at 33.3 m by a purple calcareous massive grey mottled mudstone that is 2 m thick. The lowermost 1 m of this mudstone contains carbonate nodules that range in size from 2 cm in diameter at the base and increase

too as large as 20 cm in diameter upward. Carbonate nodules abruptly disappear in the uppermost 1-meter. This unit gradually transitions at ~35.5 m in to the overlying mudstone.

The overlying unit at 35.5 m is a carbonate nodule bearing red massive mudstone with green mottles that is 1.3 m thick and contains 0.1 to 1 cm diameter nodules. A 0.1 m thick laterally discontinuous lenticular massive carbonate bed at ~37 m separates the red green-mottled mudstone from a 0.2 m thick discontinuous grey massive mudstone rich in coalified organic matter at 36.9 m. This organic matter rich mudstone is the base of a 4.6 m purple grey-mottled massive weakly calcareous smectitic mudstone. The mudstone has macroscopic slickensides and clay skins, but is overall featureless.

Petrographic examination of the purple grey-mottled mudstone reveals, bioturbated, pelleted micrite-cemented mud with some 1 mm thick spar filled veins (Fig 5G). The purple-grey mottled smectitic mudstone is separated at 44.8 m from the overlying red mudstone by a sharp contact.

The red mudstone is 1.5 m thick, massive, and non-calcareous. It contains scattered 0.2 to 2 cm diameter carbonate nodules that increase gradually upward forming a thin carbonate cemented horizon, at 46.0 m. The carbonate-cemented horizon pinches and swells varying in thickness from 10 to 30 cm at its thickest, and is laterally continuous. At 46.4 m approximately 2 m of red and white mottled non-calcareous massive mudstone separates the carbonate-cemented horizon from the uppermost carbonate unit KU-PR1-CU4 at 48.2 m.

KU-PR1-CU4 in the interval 48.2 m to 50.3 m is a carbonate bearing massive grey non-calcareous mudstone. The lowest 0.1 m is an indurated carbonate cemented mudstone. Above this carbonate cemented mudstone is 1.5 m of grey mudstone containing scattered 2 to 20 cm diameter carbonate nodules that increase in abundance gradually from 5 to 100 %, forming a welded 0.4 m thick massive lenticular carbonate unit that is laterally discontinuous but forms a distinctive slope break.

Approximately 4 m of grey massive non-calcareous mudstone that is highly altered by weathering and compaction abruptly overlies KU-PR1-CU4 at 50.3 m. This gradually transitions in to a grey and red massive mudstone that is 3 m thick. The grey-mudstone has macroscopic evidence of burrowing and slickensides. It has an unconformable contact at 56.6 m with the overlying white mottled sandy mudstone that forms the upper most unit of KU-PR1. The white mottled sandstone is 1.4 m thick and has dark grey fine-grained laminations, in the lowest 0.4 m, but is massive and coarser in the upper meter.

Price River 2 (KU-PR2) Dinosaur Quarry Section

The Price River 2 (KU-PR2) section, is approximately 1.8 km Southeast of the KU-PR1 section and measures approximately 42 meters and is bounded by two major fluvial sandstone units, with a third middle, sandstone, approximately 17 m above the basal sandstone (Fig. 4). The middle sandstone is used to arbitrarily divide the section into lower and upper sections. The top of the basal sandstone is used as the

datum for section measurement. The lower 17 m were measured through a major wash below the middle sandstone. The upper 25 meters of the section contains the College of Eastern Utah Price River II dinosaur quarry (CEU-PR2; Utah Geological Survey accession # Em372). The upper 25 meters is a composite section and the first 7.5 m were measured below CEU-PR2 on a nearby hill slope directly to the Southeast of the quarry. The upper 17.5 m were measured on the Northeast side of the quarry and on the hill slope above the quarry. A mudstone unit below CEU-PR2 that weathers to a distinctive white and is traceable over a broad area was used as the marker horizon between these two sections.

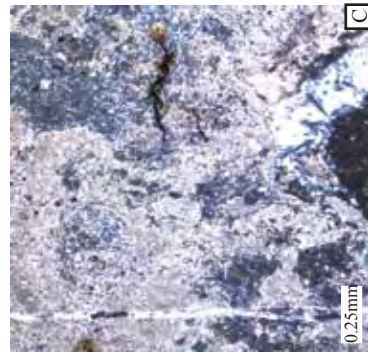
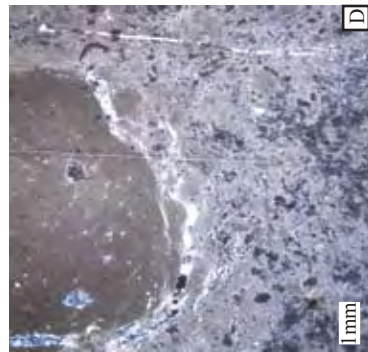
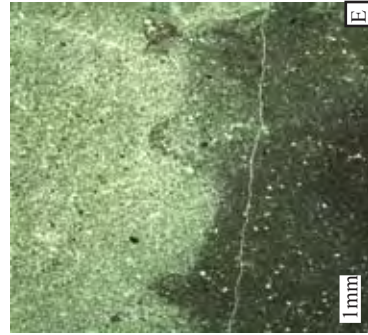
The mudstones in the upper and lower sections have interspersed carbonate-indurated and carbonate nodule-bearing units and will be referred to as carbonate units KU-PR2-CU1 to KU-PR2-CU6. Units KU-PR2-CU1 to 4 occur in the lower section and KU-PR2-CU5 and 6 in the upper section.

Lower KU-PR2 Section

The basal sandstone is a cross-laminated, fining upward, coarse to medium sand. The basal sandstone is unconformably overlain by approximately 3 m of red to purple mudstone at, with no macroscopic evidence of bioturbation, fossils or other sedimentary structures, the red mudstone grades into unit KU-PR2-CU1 at ~2.5 m.

KU-PR2-CU1 is approximately 3 m thick and contains carbonate nodules (Fig. 6), ranging in diameter from 5 to 20 cm. These carbonate nodules coalesce laterally and form horizons that inter-finger with the surrounding mudstone (Fig 6A).

Figure 6. (A) Composite image of KU-PR2-CU1, the lower most carbonate. (B) Close up of coalesced carbonate horizon, with rock hammer for scale. (C) Cross-polarized thin section image of carbonate nodule, shows micrite-cemented mudstone with rootlet and spar veins. (D) Cross-Polarized thin section, showing micrite clasts, with spar veins surrounding and spar filled voids, in a micrite-cemented matrix. (E) Thin section of mudstone surrounding carbonates, showing red and white mottling, of silty mudstone.

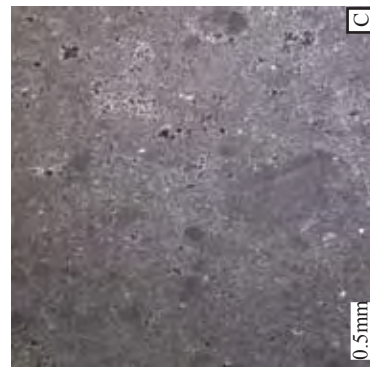
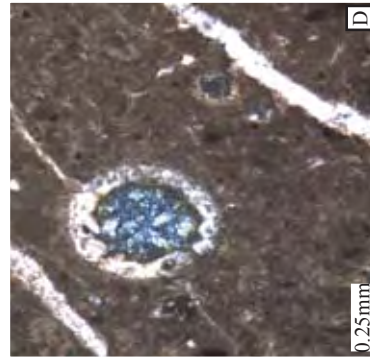
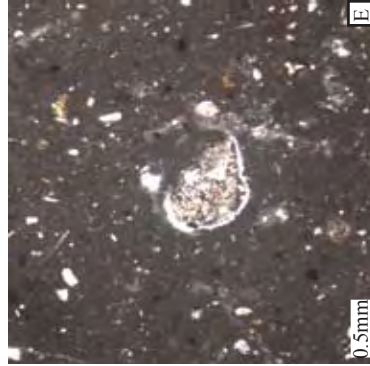


The coalesced horizons are separated from each other by a calcareous purple to red mudstone containing dispersed carbonate nodules. Carbonate nodules and horizons consist of micrite-cemented carbonates. Thin section examination reveals microscopic root traces (Fig. 6C), burrowing and bioturbation not macroscopically visible. Rounded micritic clasts are also visible in hand specimens (Fig. 6D). These clasts contain microscopic voids filled with calcite spar. Veins of sparry calcite are also found throughout the nodules and around some of the micrite clasts. The intervening mudstones are silty and mottled red and tan with evidence of microscopic bioturbation (Fig. 6E).

KU-PR2-CU1 grades upwards from ~5.5 m, into approximately 0.6 m of red/purple mudstone with interspersed carbonate nodules. Carbonate nodules increase in abundance towards the top of the mudstone unit. The upper boundary of the mudstone (6.5 m) is abrupt and is overlain by KU-PR2-CU2A and B (Fig. 7A) KU-PR2-CU2A is a 0.6 m thick horizon of compacted mudstone with micritic carbonate nodules (Fig. 7C), it extends laterally approximately 11.0 m. The mudstone surrounding the nodules is a dark purple red un-cemented mudstone. The carbonate nodules range in diameter from 10 to 20 cm. The horizon pinches out laterally and has an abrupt contact with the overlying KU-PR2-CU2B at 6.9 m.

KU-PR2-CU2B is a massive bed consisting of carbonate-cemented mudstone. KU-PR2-CU2B is lenticular extending laterally approximately 5.5 m, and at its thickest section measuring approximately 1.5 m. KU-PR2-CU2B consists of micrite-cemented mudstone. Thin section examination reveals microscopic burrowing and

Figure 7. (A) Composite image of KU-PR2-CU2A and B. Black dashed line indicates contact between the two units. (B) Close up of boundary between KU-PR2-CU2A, and B (rock hammer for scale). (C) Thin section of micritic matrix of carbonate nodule from KU-PR2-CU2A. (D) Thin section of carbonate from KU-PR2-CU2B showing charophyte in a micrite cemented matrix, with spar filled veins. (E) Thin section showing sediment filled thin-shelled ostracodes in micrite cemented matrix.



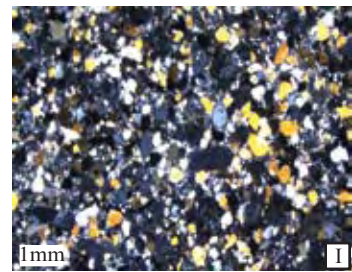
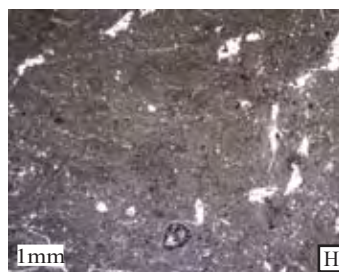
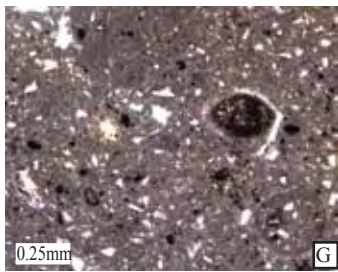
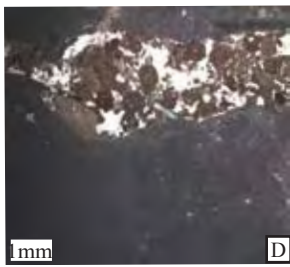
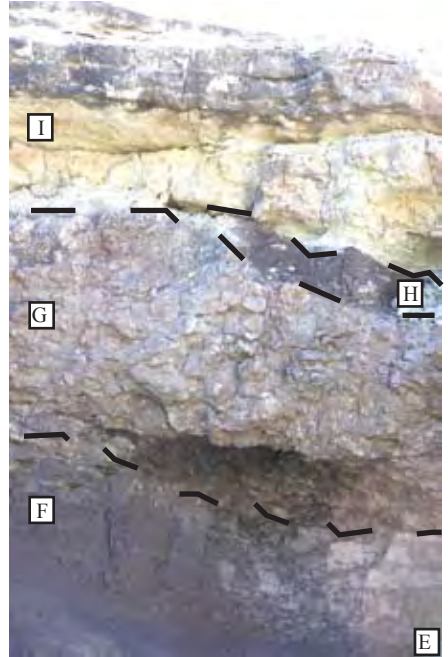
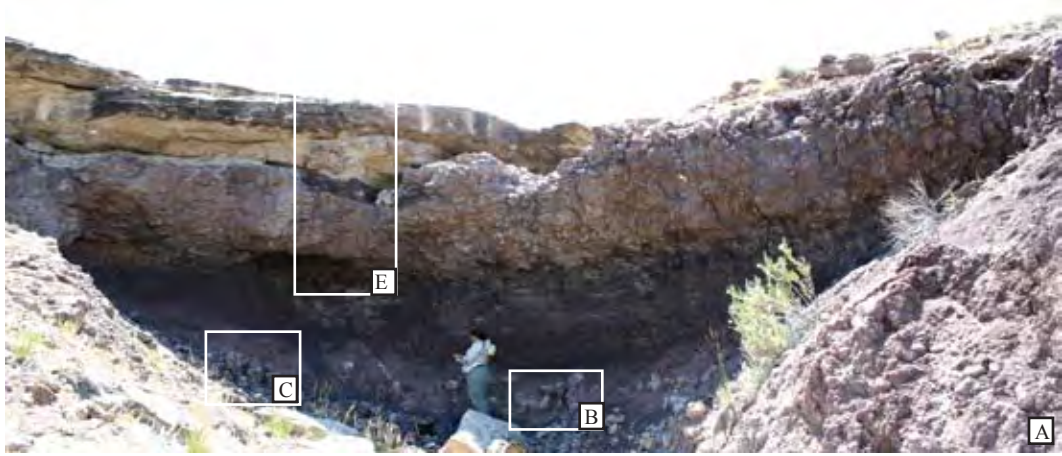
extensive bioturbation. Charophytes, and poorly preserved ostracodes are present, though rare (Fig. 7D,E). Sparry-calcite veins occur in some samples and crosscut burrows, and fossil grains (Fig. 7E). KU-PR2-CU2B is unconformably overlain by a featureless non-calcareous massive red-purple mudstone at 10.1 m. The thickness of this unit is approximately 1.5 m, however the contact with the overlying unit (KU-PR2-CU3) is covered for approximately 0.2 m.

KU-PR2-CU3 (Fig 8A, B) is at 11.6 m and is 0.7 m thick carbonate nodule bearing light purple un-cemented mudstone horizon. Carbonate nodules range in diameter from 5 to 30 cm, are purple-red, and have a columnar or U-shaped morphology (Fig. 8 B, C). The nodules are micritic and in thin section thin sparry-calcite filled veins and voids are visible. Some of the nodules contain macroscopic pellet filled voids (Fig 8D). There is an abrupt contact between this unit and the overlying silty red mudstone.

The overlying unit is a dark red-purple massive silty mudstone (Fig 8E, F) that is lenticular and 1.6 m at its thickest section. It is unconformably overlain at 13.9 m by KU-PR2-CU4.

KU-PR2-CU4 is a lenticular unit that is approximately 1.2 m thick and extends about 20 m laterally (Fig. 8A, F). KU-PR2-CU4 consists of coalesced micrite cemented carbonate nodules. Poorly preserved, thin-shelled ostracodes and bioturbation are evident in thin section (Fig. 8G). It has an abrupt contact with the overlying red-purple, mudstone.

Figure 8. (A) Image showing KU-PR2-CU3 and KU-PR2-CU4 with intervening mudstones and the middle sandstone. (B, C) Close up of KU-PR2-CU3 nodule bearing horizon. Nodule morphology is outlined with black lines in (B). (D) Thin section of carbonate nodules in KU-PR2-CU3, showing pellet filled void in micritic matrix. (E) Close up of intervening mudstone (F), KU-PR2-CU4 (G), intervening mudstone (H) and middle sandstone (I). (G) Thin section of KU-PR2-CU4 in cross-polars with sediment filled thin-shelled ostracode in a micrite cemented matrix. (H) Thin section of calcareous mudstone showing silty mud with sparry calcite filled voids. (I) Thin section of sandstone in cross polars.



Separating KU-PR2-CU4 and the middle sandstone is a massive lenticular mudstone that is approximately 0.5 m at its thickest. The mudstone is calcareous and contains microscopic scattered spar filled veins and voids (Fig. 8H). The upper surface of the mudstone is scoured and the overlying sandstone fills scours.

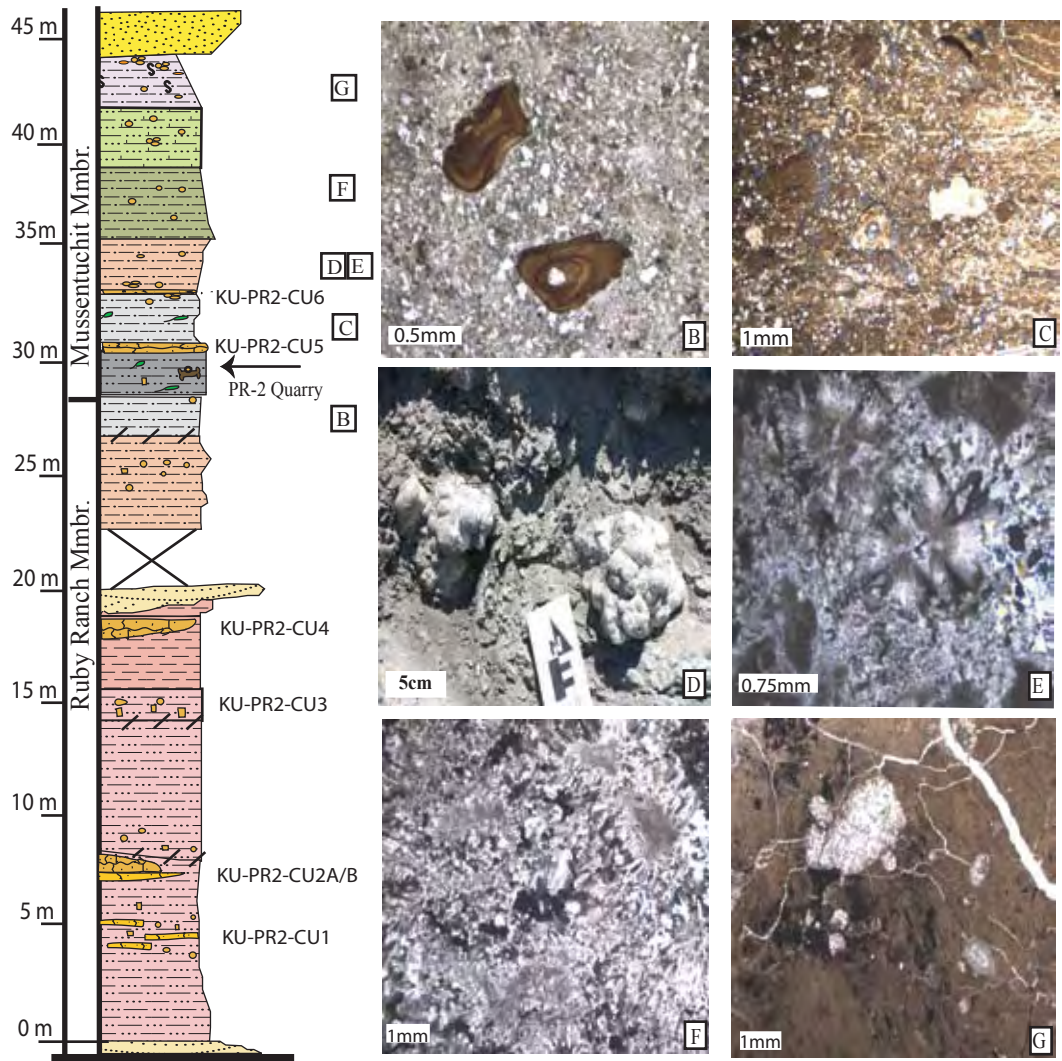
The middle sandstone is at 15.6 m and is ~1.5 m thick and lenticular. It is carbonate cemented, consisting of medium to coarse poorly sorted cross-bedded sand and (Fig. 8I) contains granule to pebble size gravel.

Upper KU-PR2 Section

There is approximately 3.5 m of colluvial cover from the top of the middle sandstone to a massive silty orange mudstone, from 20.6 to 24.5 m, that underlies the white marker horizon. The mudstone contains scattered fine sand lenses approximately 0.5 cm wide. In the uppermost 0.37 m of this unit carbonate nodules, 2 cm or less in diameter, increase dramatically from about <10% to nearly 100 % at the top of the unit. The carbonate rich nodule layer is overlain by 0.8 m of red brown non-calcareous mudstone. A sharp contact separates the brown mudstone from white weathered horizon used to anchor this section to the section at the CEU-PR2 quarry (Fig.9A).

The white weathered horizon is approximately 2.5 m thick, and is at 26.1 m. It is a laminated calcareous grey mottled sandy mudstone and contains charcoal, coalified organic matter, and dark grey rip up clasts. Petrographic examination reveals fish bioclasts, and micrite cement (Fig, 9B). The contact at 27.1 m with the

Figure 9. (A) Picture shows the sediments SE of the CEU-PR2 quarry, dashed black line shows the approximate location of the white unit used to correlate the section to the CEU-PR2 quarry, as well as the gradational boundary between the Ruby Ranch and Mussentuchit Member. The stratigraphic section shows the approximate location of thin section images presented opposite and of major carbonate units described in the text (e.g. KU-PR2-CU_x). (B) Micrite cemented sandy mudstone, with fish bioclasts (teeth?). (C) Micrite cemented sandy mudstone, with organic matter, is cross-polarized (D) Botryoidal carbonate nodules in place in grey calcareous mudstone matrix. (E) Thin section of botryoidal carbonate nodules, in cross-polars showing radial fibrous calcite, in micritic matrix. (F) Cross-polarized thin section of micritized mudstone showing fibrous calcite. (G) Thin section showing radial calcite nodules in clay rich matrix, with spar filled veins.



overlying grey-purple bone bearing mudstone that contains CEU-PR2 is abrupt. The top of the gray sandy mudstone appears to have been heavily compacted prior to deposition of the bone bearing mudstone. Dinosaur bones and large 10 cm diameter carbonate nodules unconformably rest on the top of this white-grey horizon. The horizon also appears to represent the beginning of the gradational boundary from Ruby Ranch to Mussentuchit Member.

The CEU-PR2 quarry in the interval 27.1 m to 30.7 m , has been mapped and excavated extensively by the College of Eastern Utah. Bone maps produced by CEU show two bone beds that pinch out laterally, with bones trending in a southeastward direction (Garrison et al., 2007).

These bone-bearing units are grey mudstones, with coalified organic matter and carbonate nodules. Carbonate nodules are frequently found surrounding dinosaur bones and range in size from 0.5 to 5 cm in diameter, they also occur as grape like clusters. Thin sections of the nodules show radial fibrous calcite fabrics.

Between the lower and upper quarry sections, from 29.4 m to 29.6 m is a grey calcareous sandy mudstone that contains some charcoal and coalified organic matter. A 0.5 m thick indurated carbonate mudstone (KU-PR2-CU5) forms a slope break directly above the upper bone bed. Petrography reveals nodules of radial fibrous calcite cemented by dentate to bladed calcite. Fractures and veins cut across micritic matrix and nodules. These fractures and veins are filled by a sequence of dentate to bladed and finally blocky equant calcite spar. In areas chalcedony is the last fill in fractures and veins.

A sharp contact at 33.1 m separates KU-PR2-CU5 from the overlying grey sandy calcareous mudstone. The grey sandy mudstone is 2.2 m in thickness. Thin section examination reveals coalified organic matter and charcoal in a poorly sorted micrite cemented matrix (Fig. 9C). The contact between the sandy unit and the overlying mudstone at 33.7 m is abrupt.

The mudstone is 1.5 m thick green-grey non-calcareous. Thin section examination reveals coalified organic matter in a muddy matrix with some calcite spar filled veins and bioturbation. An abrupt contact at 35.2 m separates this mudstone from the last measured carbonate indurated unit KU-PR2-CU6.

KU-PR2-CU6 is a 0.5m thick horizon consisting of continuous 0.20 m wide individual red micritic blocks. Petrographic examination reveals, sparry calcite filled veins and voids within the micrite. The contact at 35.7 m between KU-PR2-CU6 with the overlying unit is abrupt.

KU-PR2-CU6 is overlain by a 5 m thick smectite rich mudstone to the top of the section. At the base the mudstone is green with gray mottles and coarse silt grains are visible. Toward the top of the bed there is gradual increase in the amount of clay, and a gradual change in color of the unit to gray with red mottles, to red with grey mottles at the top. Clay skins are common throughout the unit. Slickensides are abundant in the uppermost 1 m of the bed. In thin section bioturbation and translocated clays are common, and spar filled veins are scattered throughout (Fig. 9G).

Botryoidal carbonate nodules ranging in size from 0.1 to 10 cm in diameter are scattered throughout the mudstone (Fig 9D). Thin section examination of these botryoids reveals that some botryoids consist only of radial fibrous calcite, while others have micritic cores surrounded by radial fibrous calcite. Micrite cements individual botryoids (Fig 9C, E). Displacive fabrics are visible around the nodules, and translocated clays commonly surround the nodules.

Price River 3 (KU-PR3) and 4 (KU-PR4)

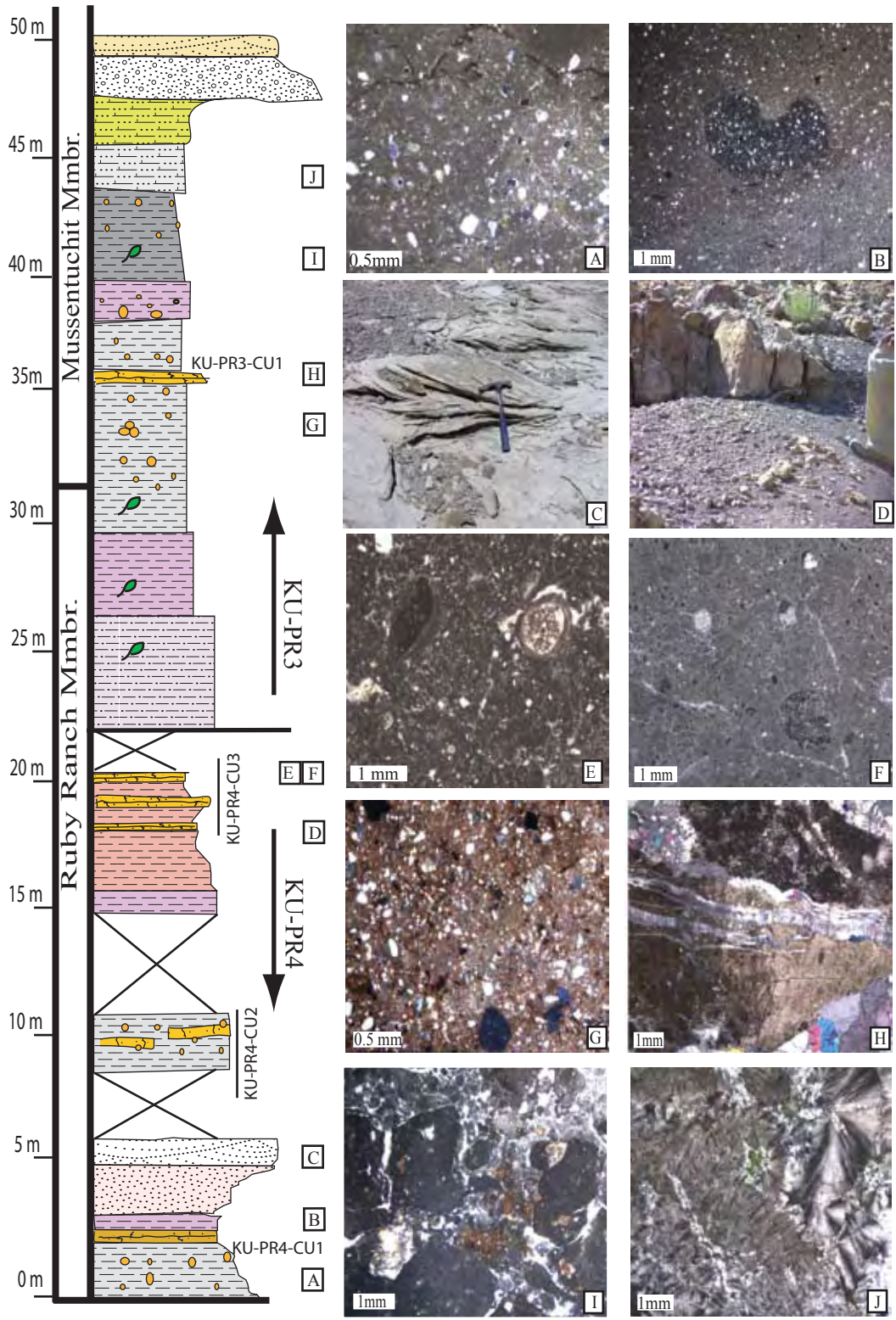
KU-Price River 3 and KU-Price River 4 are the upper and lower sections, respectively forming a composite section that measures approximately 50 m. The section is located approximately 2.3 km Southeast of KU-PR1. The lower half of the section KU-PR4 is capped by a thick indurated carbonate mudstone, (KU-PR4-CU3) which forms a slope break separating KU-PR4 from KU-PR3 at 20.5 m.

Price River 4 (KU-PR4): Lower Section

KU-PR4 measures approximately 21 m and includes 3 major carbonate indurated units. KU-PR4-CU1 represents the lower most carbonate unit and KU-PR4-CU3 is the upper most carbonate unit that forms the slope break between KU-PR4 and KU-PR3.

The lower most part of this section is a carbonate nodule-bearing grey and purple mottled mudstone that measures approximately 1.7 m. The mudstone matrix is non-calcareous though small carbonate nodules 0.1 to 1 cm are present through out

Figure 10. KU-PR3/4 stratigraphic section showing approximate location of images on the right and of carbonate units described in the text (e.g. KU-PR3/4-CUx). (A) Cross-polarized petrographic image of micrite cemented silty mudstone (B) Thin section of silty mudstone with U-shaped burrow (C) Rippled sandstone, ripples trend in a SE direction. (D) Thin section showing cross section through burrow and clasts in a pelleted matrix. Image is cross-polarized. (E) Laterally pinching out carbonate bed. (F) Cross-polarized thin section showing sponge spicule and sediment filled ostracodes in a micritic matrix. (G) Cross-polarized thin section showing ostracodes in a silty mudstone matrix. (H) Thin section showing Micritic matrix with late sparry calcite filled veins. (I) Thin section showing clotted fabric, with sparry calcite filled voids. (J) Cross-polarized thin section showing, radial fibrous calcite in a micritic matrix.



the unit. The abundance and size of nodules increases from a few millimeters in diameter to greater than 10 cm in diameter towards KU-PR4-CU1. Thin sections of the mudstone reveal microscopic root traces and bioturbation (Fig. 10A).

There is a sharp boundary between the grey-purple mudstone and KU-PR4-CU1 at 1.7 m. KU-PR4-CU1 is a 0.5 m coalesced carbonate nodule unit. Nodules are 5-15 cm in diameter and are partially cemented in to a single horizon. Un-cemented voids contain calcareous purple mudstone that is similar to overlying mudstone. Petrographic examination of nodules reveals a micritic matrix with spar filled veins. A purple mudstone abruptly overlies KU-PR4-CU1 at 2.2 m.

The mudstone is approximately 0.9 m thick and is a mottled purple massive mudstone, with interspersed carbonate nodules. The mudstone is lenticular, and petrographic examination reveals micritic cement, and microscopic burrows and bioturbation (Fig 10B.) The overlying sandstone fills scours in the mudstone with some carbonate nodules protruding from the very top of the mudstone in to the sandstone.

The sandstone interval from 2.6 m to 6.5 m is a fining upward, fine to medium cross-laminated, rippled white-pink sandstone. It is carbonate cemented and ripples indicate a southeastward paleocurrent direction (Fig 10C).

There is significant colluvium (~2.5 m) between this thick sandstone and the green to purple mottled mudstone at 9.2 m that contains KU-PR4-CU2. This unit is approximately 2 m thick and the mudstone matrix is calcareous and massive with interspersed carbonate nodules that grade in to interfingering lenticular carbonate

cemented mudstones. The individual lenses are approximately 0.25 m thick and extend for approximately 1 to 2 m laterally before pinching out. Examination of thin sections from this unit reveals, a micritic matrix with some tan and dark purple micritic clasts and some small, (<0.25 mm) voids filled with sparry calcite, as well as evidence of bioturbation. Approximately 4 m of colluvium, from 11.4 m to 15.3 m separates this interval from the next unit.

Approximately 1.3 m of purple to red non-calcareous massive mottled featureless mudstone overlies the covered section. There is a gradational transition between 16.4 m to 16.7 m from mudstone into the overlying carbonate unit KU-PR4-CU3.

KU-PR4-CU3 is a 4 m thick, series of lenticular carbonate beds in a red to orange mudstone matrix. The mudstone is a calcareous massive mudstone. The carbonate lenses measure approximately 0.5 m at their thickest section, and pinch out laterally (Fig 10D). Petrographic examination of the carbonate nodules reveals a clotted micritic texture, with 1 mm in diameter, micritic clasts, pellets, poorly preserved sponge spicules, ostracodes and charophytes (Fig. 10E, F).

Price River 3 (KU-PR3): Upper Section

KU-PR3 measures approximately 27 m and contains one indurated carbonate unit KU-PR3-CU1. There is approximately 1.3 m of cover from the top of KU-PR4-CU3 (20.8 m) and the base of KU-PR3 (22.1 m).

The lower most unit of KU-PR3 is a grey to purple mottled silty mudstone, and is approximately 4 m thick, in the interval 22.1 m to 26.2 m. The mudstone is massive and non-calcareous, with some coalified organic matter. It grades in to a finer grained purple to grey mottled massive mudstone at ~26.0 m. There are 3 m of this purple-grey mottled mudstone. It is non-calcareous and contains some coalified organic matter. The contact between the purple-grey mottled mudstone and the overlying grey smectitic mudstone, at 28.8 m is sharp and appears to be the beginning of the transition from Ruby Ranch to Mussentuchit Member.

The grey smectitic mudstone is massive and generally featureless extending from 28.8 m to 35.1m, to the base of KU-PR3-CU1. The mudstone has variable amounts of calcium carbonate and contains dispersed carbonate nodules that range in size from 0.1 to 5 cm, and some coalified organic matter (Fig10.G). The contact at 35.1 m between the mudstone and KU-PR3-CU1 is abrupt.

KU-PR3-CU1 is a 0.5 m thick, and is grey to purple mottled. It is laterally extensive, forming a slope break. Petrographic examination of thin sections reveals micrite-cemented mudstone, with scattered spar filled veins (Fig 10H). The contact at 35.6 m between the micrite-cemented mudstone and the overlying silty mudstone is abrupt.

Approximately 2.2 m of non-calcareous massive silty grey mudstone overlies KU-PR3-CU1. The mudstone has dispersed 0.1 to 4 cm diameter carbonate nodules. Thin sections of these nodules show micrite with some spar filled veins. The mudstone is massive with some microscopic evidence of bioturbation. This mudstone

gradually transitions in to a purple-grey calcareous mudstone that is 1.2 m thick and contains large 1 to 10 cm diameter carbonate nodules. Petrographic examination of thin sections reveals microscopic roots and micritic cement. As well as some < 1 mm thick spar filled veins. The purple-grey mudstone gradually transitions into the overlying dark grey non-calcareous mudstone.

The dark grey mudstone is massive and approximately 3 m thick with dispersed 0.3 to 5 cm diameter carbonate nodules. Thin sections show bioturbated mud with small micritic and radial fibrous calcite carbonate nodules and coalified organic matter. The contact at 43.4 m, between the dark grey mudstone and the overlying grey claystone is abrupt. The claystone is 2.8 m thick and slightly calcareous. It is massive and mottled grey and light grey, and has some slickensides, the amount of clay decreases gradually towards the top of the bed. The grey mudstone gradually transitions in to a yellow claystone at approximately 46.2 m. The yellow claystone is approximately 1 m thick, massive and highly weathered. It unconformably underlies the conglomerate at 47.1 m.

The conglomerate is 1.4 m, tan and can be split in to two distinctive beds. The lower interval 47.1 m to 47.7 m coarsens upward, from pebble and granular size clasts at the base to cobbles at the top of the bed, while the upper interval from 47.7 m to 48.4 m is poorly sorted, un-graded cobbles, pebbles and granules in a coarse sand matrix. Above the conglomerate is tan sandstone that unconformably rests on the conglomerate. The sandstone is tan, and carbonate cemented, it is well sorted, fining upward, fine to medium, cross laminated sand.

$\delta^{13}\text{C}_{\text{org}}$ and Total Organic Carbon Chemostratigraphy

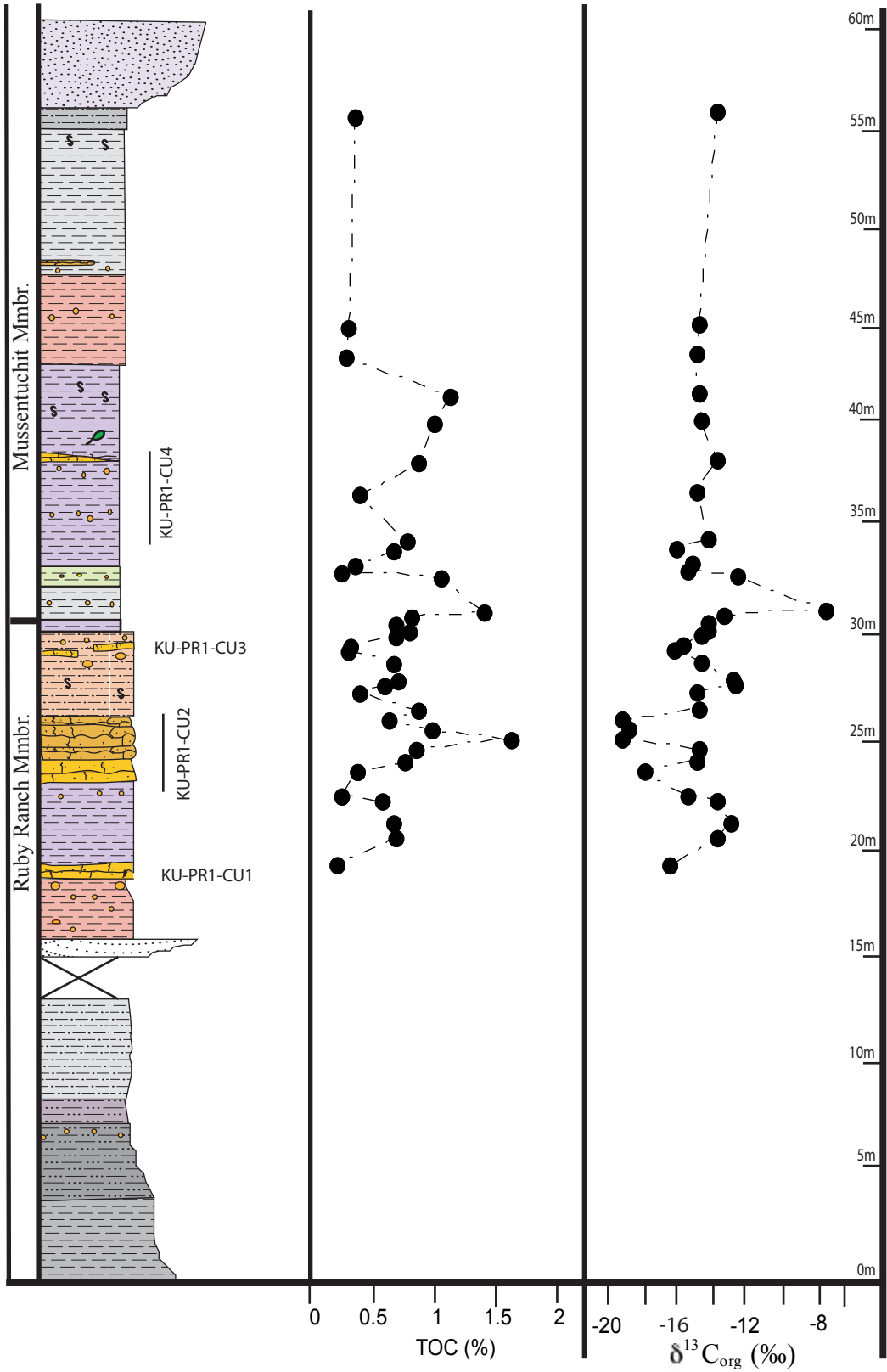
KU-PR1

The TOC and $\delta^{13}\text{C}_{\text{org}}$ chemostratigraphic profiles start approximately 18.8 m above the base and extend to approximately 55.1 m (Fig. 11, Appendix D). The maximum value for $\delta^{13}\text{C}_{\text{org}}$ is -7.8 ‰, at 31.0 m and the minimum value of -19.5 ‰ at 25.8 m. The maximum TOC value of ~1.6% occurs at 24.8 m and the minimum value, 0.2%, at the base of the section (18.8 m).

The TOC profile for KU-PR1, (Fig.11) shows a ~0.5% increase from 0.2% at 18.8 m to 0.7% at 20.1 m. This increase in TOC is followed by a ~0.5% decrease from 0.7% (20.7 m) to 0.2% (22.0 m). A 1.4% increase in TOC from 22.0 m to 24.8m follows, with the maximum TOC value of 1.6% reached at 24.8 m. A gradual 1.3% decrease occurs over the next 2.3 m (24.8 m to 27.1m), reaching a value of 0.4% followed by a 0.3% increase to 0.7% from 27.1m to 28.6 m, a 0.4% decrease to 0.3% occurs from 28.6 to 29.1m. Through the next 4 m to 32.7 m we see a 1.1% increase in TOC to 1.4%, which then decreases by 1.2% from 31.0 m to 33.0 m. The TOC then gradually increases over 8 m to 1.1% TOC. The top if this section (41.6 to 55.1 m) is marked by a decrease and stabilization of TOC at ~0.3%.

The $\delta^{13}\text{C}_{\text{org}}$ chemostratigraphic profile has a 3‰ increase in the $^{13}\text{C}_{\text{org}}$ from -16.7‰ to -13.2‰ over ~2 m, this is then marked by a steep -5‰ decrease at 23.3 m. The $\delta^{13}\text{C}_{\text{org}}$ then increases by 3‰ to -15.1‰ from 23.3 m to 23.8 m, then decreases sharply to -19.5‰ from 23.8 to 25.8 m. A 4‰ increase in $\delta^{13}\text{C}_{\text{org}}$ to -13.0 ‰ (27.4 m)

Figure 11. Chemostratigraphic profile of KU-PR1 showing a curve for TOC (%) and a curve for $\delta^{13}\text{C}_{\text{org}}$ (‰) against depth from base of section. Figure also shows the location of major carbonate units.



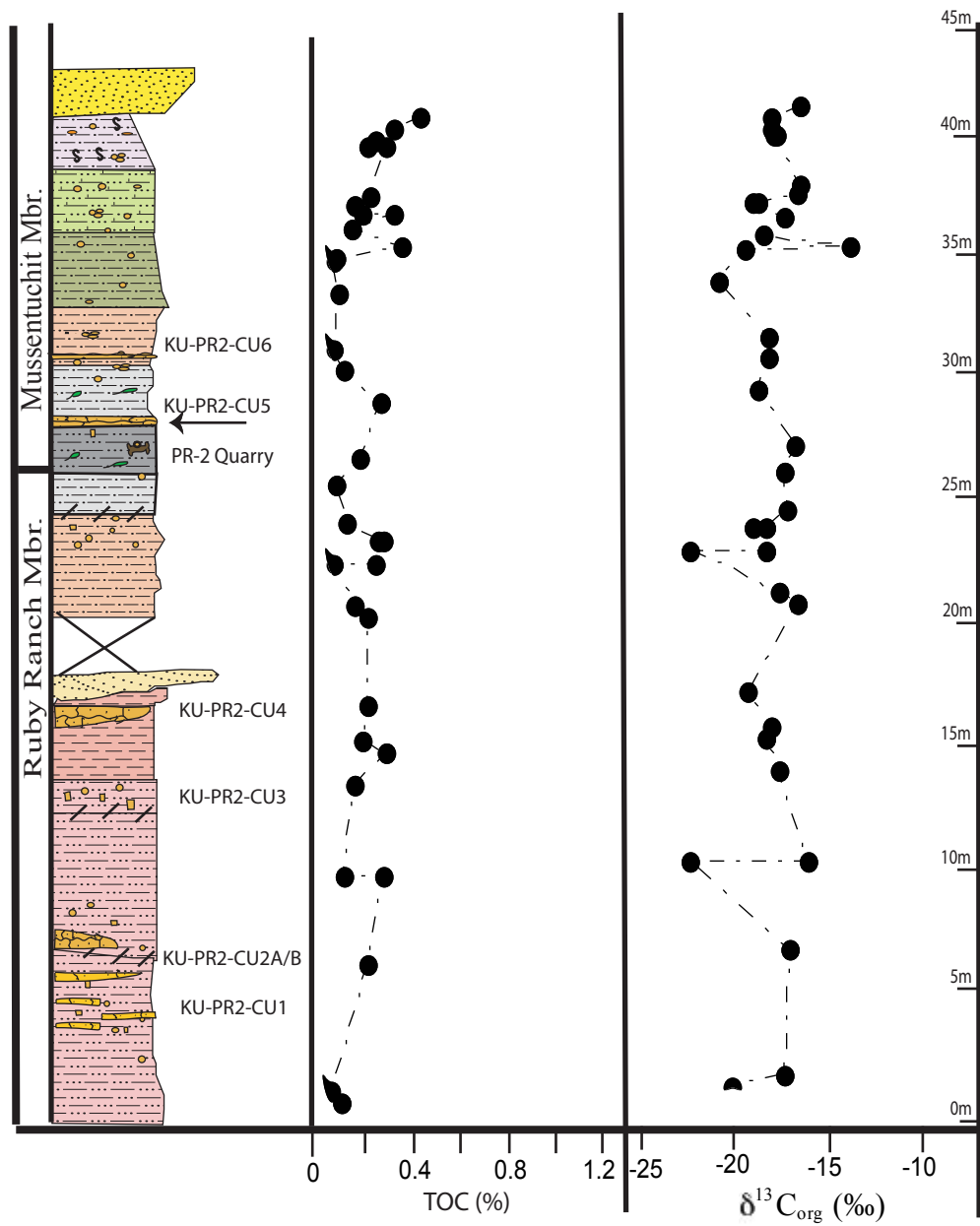
follows this decrease. The $\delta^{13}\text{C}_{\text{org}}$ values decrease to -16.6 ‰ from 27.4 m to 29.0 m. A 6‰ increase in $\delta^{13}\text{C}_{\text{org}}$, occurs from 30.7 m to 31.0 m and is followed by a 8 ‰ decrease over ~2 m (31.0 m to 33.0), which stabilizes to values averaging ~ -15.0‰ from 33.0 m to 55.1m at the top of the section.

KU-PR2

The TOC and $\delta^{13}\text{C}_{\text{org}}$ chemostratigraphic profiles for KU-PR2, (Fig. 12, Appendix E) extends from approximately 1m above the base to approximately 41.0 m. The minimum TOC value is 0.04 % at 1.5 m above the base and the maximum value is 0.4% at 41.0 m. The TOC content for KU-PR2 is relatively low with the average value around 0.2% and variability limited to $\pm \sim 0.2\%$. The minimum $\delta^{13}\text{C}_{\text{org}}$ value is -22.3 ‰ at 22.8 m with a maximum value of -13.8‰ at 35.2 m.

The $\delta^{13}\text{C}_{\text{org}}$ at the base of the section (1 m) is -20.1‰, which increases by ~3‰ from 1.0 to 1.5 m to ~ -17.0‰. From ~1.0 to 10.1 m the $\delta^{13}\text{C}_{\text{org}}$ decreases to -22.2‰, this is followed by an increase to ~ -17.6 ‰ from 10.1 m to 13.9 m. The $\delta^{13}\text{C}_{\text{org}}$ values decrease by 2‰ and stabilizing at an average value of ~ -17.9‰ from 13.9 m to 22.8 m. The $\delta^{13}\text{C}_{\text{org}}$ in this interval (13.9 m to 22.8m) varies by $\sim \pm 2$ ‰. At 22.8 m the $\delta^{13}\text{C}_{\text{org}}$ decreases to -22.3‰ then stabilizes at an average $\delta^{13}\text{C}_{\text{org}}$ of ~ -18.3 ‰ ± 2 ‰, from 23.7 m to 35.1 m. The $\delta^{13}\text{C}_{\text{org}}$ increases in the interval 35.1 m to 35.3 m, to -13.8 ‰. The $\delta^{13}\text{C}_{\text{org}}$ then decreases by 4.5‰ to -18.3‰ in the interval 35.2m to 35.7 m then stabilizes with an average value of ~17.6 ‰, ± 1 ‰ from 35.7 m to 41.0 m, at the top of the section.

Figure 12. Chemostratigraphic profile of KU-PR2 showing a curve for TOC (%) and a curve for $\delta^{13}\text{C}_{\text{org}}$ (‰) against depth from base of section. Figure also shows the location of major carbonate units.

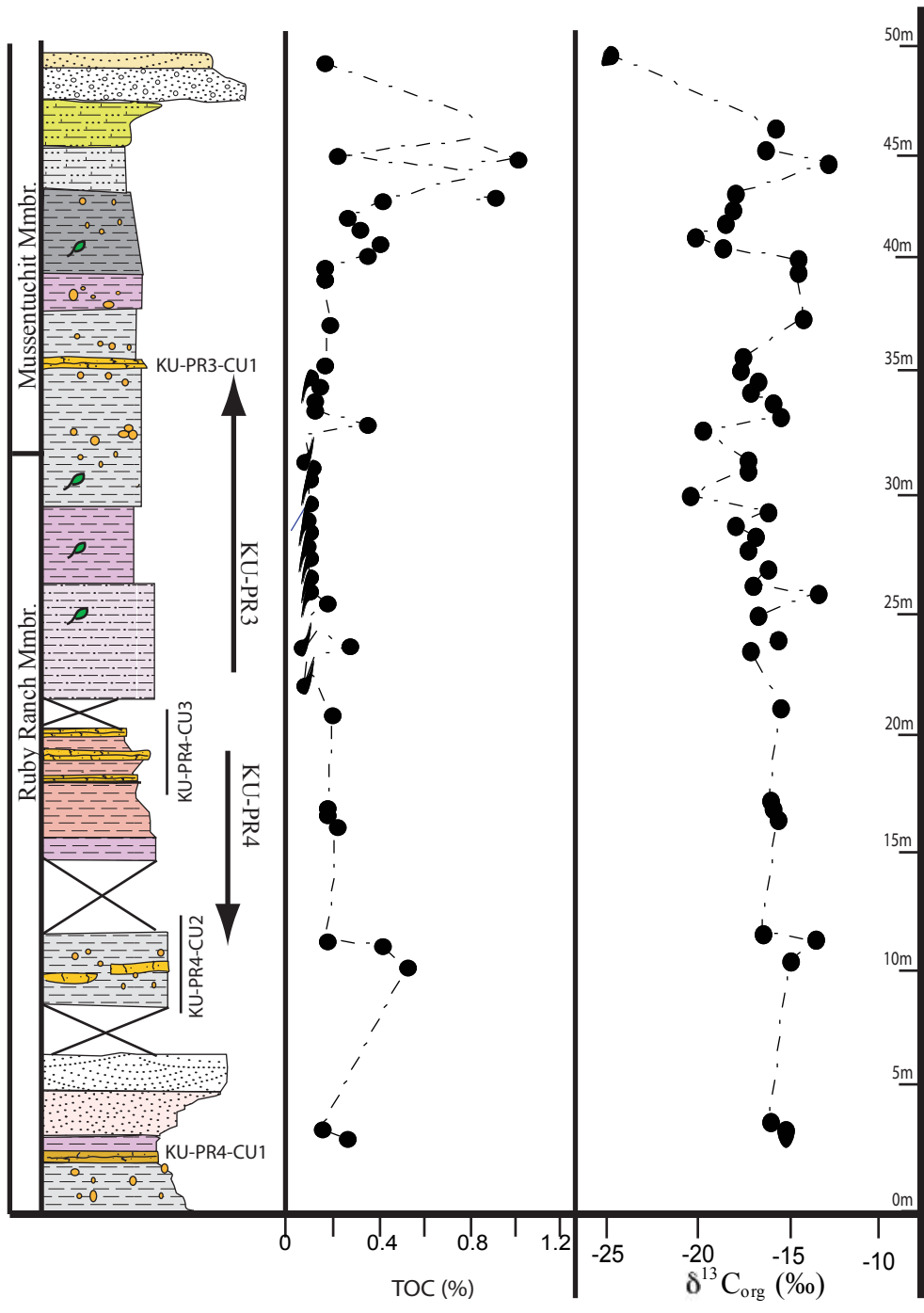


KU-PR3/4

The $\delta^{13}\text{C}_{\text{org}}$ and TOC profiles for this section extend from approximately 2.3 m to 49.0 m, (Fig. 13, Appendix F). The minimum TOC value is 0.05% at 24.9 m and the maximum value is 1.0% at 46.2 m. In general the TOC profile for KU-PR3, from the base of the chemostratigraphic profile to ~42.0 m is fairly stable, with TOC values varying by $\sim \pm 0.2\%$ from an average value of 0.2%. From 43.4 m to 44.6 m the TOC content increases to 0.9 %, then decreases to 0.2% from 44.6 m to 45.3 m. The TOC increases to 1.0% in the interval 45.3 m to 46.2 m then decreases from 46.2 m to 49.4 m to 0.1% at the top of the section.

The minimum $\delta^{13}\text{C}_{\text{org}}$ is -24.8 ‰ at 49.4 m with a maximum value of -12.8‰ at 44.6 m. The $\delta^{13}\text{C}_{\text{org}}$ chemostratigraphic profile for KU-PR3, shows fairly constant $\delta^{13}\text{C}_{\text{org}}$ values of $\sim -15.6\text{‰} \pm 2\text{‰}$ from 2.2 m to 24.9 m, whereby the $\delta^{13}\text{C}_{\text{org}}$ increases by 3 ‰ to -13.4‰ in the interval 24.9 m to 25.7 m. The $\delta^{13}\text{C}_{\text{org}}$ decrease to -16.9‰ from 25.7m to 26.2m and stabilizes at $\delta^{13}\text{C}_{\text{org}}$ values of $\sim -16.6\text{‰} \pm 1\text{‰}$ from 26.2 m to 29.4 m. The $\delta^{13}\text{C}_{\text{org}}$ values decrease to -20.4‰, from 29.4 m to 30.0 m, then increases from 30.0 m to 33.0 m, to -19.7‰. From 33.0m to 33.5m the $\delta^{13}\text{C}_{\text{org}}$ increases to $\sim -16.7\text{‰} \pm 1\text{‰}$ and remains stable in the interval 33.5m to 36.1 m. From 36.1 to 37.9 m the $\delta^{13}\text{C}_{\text{org}}$ increases to $\sim -14.1\text{‰}$ then stabilizes at an average value of -14.3‰ from 37.9 m to 40.4m. In the interval 40.4 m to 41.5m the $\delta^{13}\text{C}_{\text{org}}$ decreases to -20.1‰, then increases over 0.6 m to -18.4‰ stabilizing at average values of -18.1‰ from 42.1 m to 43.4 m. The $\delta^{13}\text{C}_{\text{org}}$ values from 43.4 m to 44.6 m increase to -

Figure 13. Chemostratigraphic profile of KU-PR3/4 showing a curve for TOC (%) and a curve for $\delta^{13}\text{C}_{\text{org}}$ (‰) against depth from base of section. Figure also shows the location of major carbonate units.



12.8‰ then decrease gradually to -24.8‰ from 44.6 m to 49.4m at the top of the section.

DISCUSSION

Facies Distribution

The three measured sections all contain facies characteristics of distal and proximal floodplain deposits as well as fluvial channel deposits. There are several similar, but distinctive units in all three sections these include; channel fill sandstone, mudstone and calcretes; palustrine/lacustrine calcretes; and oxidized and gleyed paleosols with carbonate nodules and carbonate horizons. Paleosol and palustrine/lacustrine facies occur between fluvial channel successions.

Fluvial Channels

The fluvial channels and abandoned channels are typically characterized by sandy and muddy channel fills as well as some conglomeratic lenses. With a range of grain and clast sizes, in well and poorly sorted matrices. These channels are sometimes carbonate cemented forming lenticular calcrete beds that express some paludal characteristics such as charophytes, ostracodes and bioturbation (e.g. KU-PR2-CU2B and KU-PR2-CU4), suggesting that carbonate cementation of mud may have occurred during channel abandonment as the channel avulsed.

During channel abandonment, these channels may have either filled with over-bank deposits, including mud and organic debris that would be flushed in to the

abandoned channel during flooding events in the adjacent channel or stream. However it seems more likely that these channels were choked with muddy sediment, plugging the channel. As at KU-PR2-CU3/4 (Fig. 8) a lenticular mud is present that does not show any evidence of pedogenesis, perhaps as a result of limited or no subaerial exposure, and high rates of sedimentation as it plugged the fluvial channel (Demko et al., 2004; Kraus, 1987). These sediment-choked channels would have retained water for periods of time owing to the relatively low gradient of the channels, and water may have leached in to them from the surrounding landscape as well as from the groundwater table. This ponding of water would allow for paludal features such as bioturbation, rooting and inhabitation by organisms such as ostracodes and charophytes to take place. Gradual evaporation of this water would lead to the concentration of carbonate, eventually leading to the precipitation of calcium carbonate into the mud. As most of these channel carbonates appear to be micritic we would assume that this process occurred relatively rapidly, reflecting relatively arid periods during formation. These channels would form lenticular calcretes that reflect the shape of the channel in which they formed as well as doming as the carbonate cementation displaces sediment (Alonso-Zarza, 2003; McLaren, 2004; Nash and Smith, 1998). As in the case of KUI-PR2-CU4, these channels may later have been reoccupied. Carbonate nodules beneath these channel carbonates (KU-PR-CU2A, KU-PR2-CU-3 and KU-PR4-CU1 (nodules at top of mudstone unit) may represent carbonate filled burrows. These nodules show burrow morphology such as U-shapes, and horizontal and vertical cylindrical columns (Hasiotis, 2002). Organisms may have

occupied and nested in the muddy bottom of choked channels, during channel abandonment. These burrows may have been open as the channel calcrite formed, allowing carbonate to penetrate and fill these voids, cementing and preserving the morphology.

Channel fills are frequently stacked, and suggest a high variability in the channel load, from fine-grained mud to mixed pebbles and cobbles.

Palustrine/Lacustrine Calcretes and Sediments

Facies indicative of palustrine and lacustrine environments are common through out all three units. These facies typically consist of micritic and pelloidal mudstones, with bioturbated, clotted textures, ostracodes and many contain charophytes. These palustrine and lacustrine carbonates are part of a fluvial system formed as the channel migrated across its floodplain. These bodies may have received water supply either by run-off, episodic inflow from adjacent channels and streams, or groundwater recharge (Sanz et al., 1995).

The thickness and lateral extent of KU-PR1-CU2 (Fig 5B, E) suggests that this unit represents a long lived lake system, The CEU-PR2 quarry and overlying carbonate horizon KU-PR2-CU5 is believed to represent an oxbow like-lake, with over bank deposits filling it, this could include dinosaurian material washing into the channel as active channel flooded.

KU-PR1-CU2 and KU-PR4-CU3 (Fig.10F), consisting of stacked lenses with limited lateral extent and evidence of episodic exposure and sometimes pedogenesis

suggestive of a palustrine environments (Alonso-Zarza, 2003; Sanz et al., 1995).

These were most likely short-lived ponds with carbonate precipitating at the end of a wet season.

Paleosols

Paleosols in the Ruby Ranch Member, have large carbonate nodules (1 to 20 cm diameter) and carbonate horizons associated with them, they are highly oxidized red, and typically are massive and featureless (Fig. 6). The carbonates tend to be micrite and micrite cemented mudstone. The abundant carbonate nodules and thick calcrete horizons suggest that these paleosols were associated with a drier climate with intermittent wet periods.

Paleosols in the Mussentuchit Member in all three sections, are better developed (more mature) than those in the Ruby Ranch. They tend to be clay rich, gleyed, with evidence of bioturbation, roots and clay translocation, and have small carbonate nodules associated with them, and carbonate horizons when present are thin. The carbonate nodules and horizons are typically radial fibrous calcite, as well as fibrous and dentate calcite with micritic calcite coating. The gleying, translocated clays, and the lower carbonate content of these paleosols suggest that these paleosols were associated with a much wetter climate regime.

Paleoenvironmental Interpretation

In general section KU-PR1 appears to be dominated by lacustrine and palustrine environments, a single sandstone unit is found towards the base of this section and the mudstones in the section are generally massive and interbedded with thick palustrine and lacustrine deposits. This association suggests that the section is part of the more distal floodplain, and is not affected by high variability in deposition from a nearby channel.

Sections KU-PR2 and KU-PR3/4, show a mixture of facies, with more variability in mudstone composition and extensive paleosols and pedogenic carbonate development, as well as a higher abundance of palustrine deposits. Both sections have major sandstones at the base and top of the section, as well as the presence of at least three abandoned channel fills (KU-PR2-CU2B, KU-PR2-CU4 and the CEU-PR2 quarry) at section KU-PR2, indicating close proximity to the active channel.

This interpretation of floodplain deposits including, palustrine, lacustrine, paleosol facies with channel deposits, in a xeric moisture regime, is consistent with previous interpretations of sediment packages in the Cedar Mountain Formation (Currie, 1998; Garrison et al., 2007; Nelson and Crooks, 1987; Sprinkel et al., 1999)

Chemostratigraphic Interpretation

The $\delta^{13}\text{C}$ of modern C_3 terrestrial plants fall within a range of -23‰ to -34 ‰, with an average of -27‰, (Smith and Epstein, 1971; Tieszen, 1991). Bocherens et al. (1993) indicated that the range for Mesozoic terrestrial plants is -28 to -20 ‰. The

overall $\delta^{13}\text{C}_{\text{org}}$ values measured in this study are relatively high in comparison and well above the range for C_3 values of modern or Mesozoic plants from mesic environments (Bocherens et al., 1993; Grocke et al., 1999; Robinson and Hesselbo, 2004). However, under water and/or temperature stressed conditions (i.e. hot and xeric) $\delta^{13}\text{C}$ values can be relatively heavier and in the -20 ‰ range (Bocherens et al., 1993; Tieszen, 1991). Even so these end member values are still lower than the average $\delta^{13}\text{C}$ values for any of the measured sections. As these are fluvial systems, the bulk organic matter represents input from both terrestrial organic matter as well as aquatic organic matter. Freshwater plants have $\delta^{13}\text{C}$ values ranging from -11 ‰ to -36 ‰ and are much more sensitive to variability in atmospheric carbon dioxide (Farquhar et al., 1989). During drier conditions aquatic plants tend to have relatively heavy $\delta^{13}\text{C}$ values due to change from CO_2 to HCO_3^- metabolism possibly enhanced by exchange with atmospheric CO_2 (Leng et al., 2006). Under the xeric and warm conditions that prevailed in this region we would expect terrestrial and aquatic vegetation to have relatively heavier carbon isotopic compositions than in equivalent mesic environments.

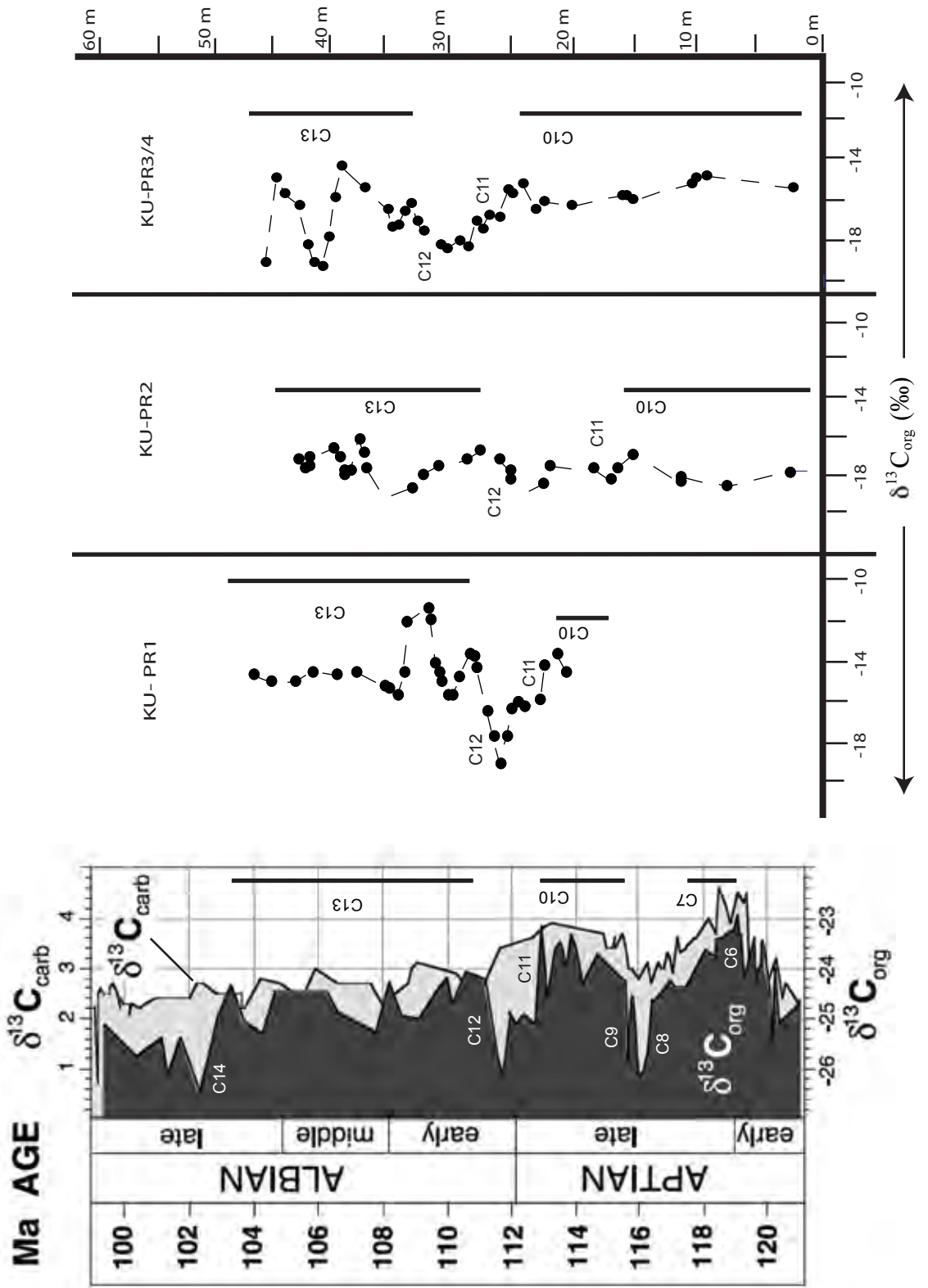
Differences in the absolute values of $\delta^{13}\text{C}_{\text{org}}$ between KU-PR1 with the relatively heavier $\delta^{13}\text{C}$ values of KU-PR2 and KU-PR3/4 are most likely a result of difference in dominant biota contributing to the bulk organic carbon. Thus the major difference between these units can be attributed to an abundance or dominance of aquatic vegetation in the palustrine to lacustrine environments that are more common

in KU-PR1. Greater contribution by terrestrial vegetation results in somewhat lighter $\delta^{13}\text{C}$ values at KU-PR2 and KU-PR 3/4.

Recent studies by Burton et al. (2006) constrain the maximum age of the section in the vicinity of KU-PR2 to a range from 116 Ma to about 109 Ma based on single crystal dates on detrital zircons. The age of the Mussentuchit is constrained by double dated single detrital zircons using (U-Th)/He and U-Pb from Muddy Creek, (Appendix H), in East Central Utah, with a basal age of 104 ± 2.7 Ma. While $^{40}\text{Ar}/^{39}\text{Ar}$ dated ash beds from Mussentuchit Wash, in Central Utah provide an upper age limit of 96.7 ± 0.5 (Garrison et al., 2007) These known ages for rocks in the Cedar Mountain Formation, specifically in the area of study, constrain chemostratigraphic correlations to carbon excursions occurring during the Aptian-Albian, specifically carbon isotope excursions C10 to C13 as defined by Bralower et al. (1999) (Fig 14). Correlations among sections and with Bralower et al. (1999) profiles are based on a three point moving average of the $\delta^{13}\text{C}$ data. Due to changing input of terrestrial vs. aquatic organic matter the magnitude of the various $\delta^{13}\text{C}$ excursions is different at any given point in time and space (Fig. 15). Correlation is based in part on the magnitude of excursions but more importantly on the structure of the chemostratigraphic profile. Apparent differences in the duration of the shifts are due to differences in sedimentation rate.

At sections KU-PR2 and KU-PR3/4 the $\delta^{13}\text{C}_{\text{org}}$ profiles are relatively constant at the base and followed by a negative excursion. The stable portion of this $\delta^{13}\text{C}_{\text{org}}$ profile is correlated with the C10 interval with the termination selected as the first

Figure 14. Three point moving average for $\delta^{13}\text{C}_{\text{org}}$ (‰) for KU-PR1, KU-PR2 and KU-PR3/4, correlated with the mid-Cretaceous record for Carbon Excursions from 120Ma to 100 Ma, as recorded by $\delta^{13}\text{C}_{\text{org}}$ and $\delta^{13}\text{C}_{\text{carb}}$ carbon isotopic records (adapted from Bralower et al. 1999; Leckie et al., 2002). Note KU-PR1, KU-PR2 and KU-PR3/4 are depth profiles while the mid-Cretaceous record is chronological.



positive excursion, with values of $\sim 14.0\text{‰}$, that is followed by a small 2‰ negative step in the Price River sections (Fig. 14). The basal record at KU-PR1 only captures the final positive excursion at the termination of the C10 interval.

At KU-PR1, a 6‰ stepwise negative shift follows this final stage of C10, at KU-PR2 and KU-PR3/4 this is less intense, $\sim 4\text{‰}$ though still a stepwise negative shift. This negative-stepwise shift is correlated with the global negative carbon excursion C11.

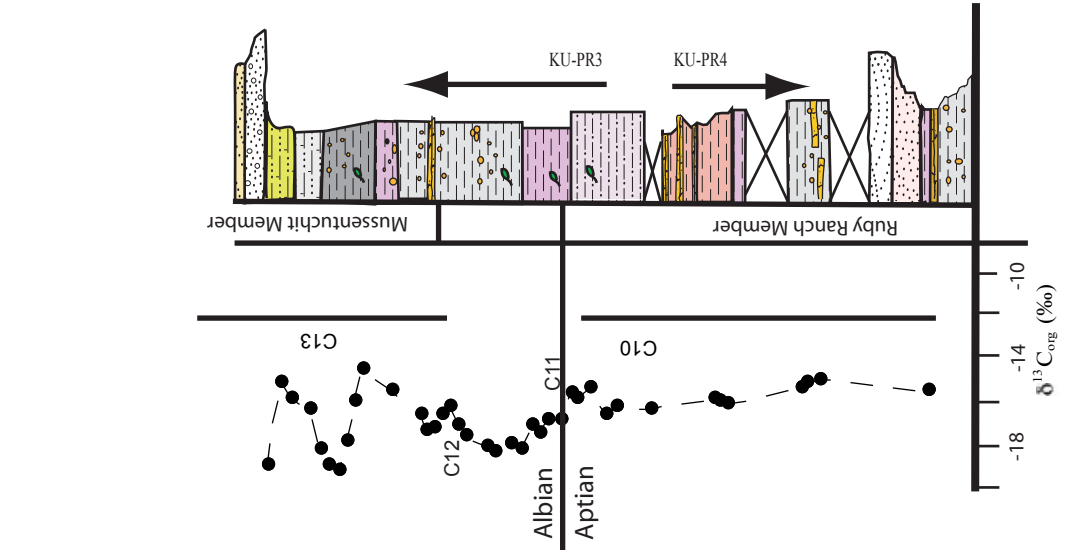
A sharp 6‰ positive shift at KU-PR1 follows the negative shift correlated as C11. At KU-PR2 and KU-PR3/4 this positive shift is of lesser magnitude and approximately 3‰ . This positive shift is correlated to the C12 positive excursion of Bralower et al. (1999) (Fig. 14). The final part of this chemostratigraphic profile is marked in KU-PR1 and KU-PR2 by an approximately 2‰ negative shift, followed by 4‰ positive shift at KU-PR1 and 3‰ at KU-PR2 and KU-PR3/4. This segment and overlying data are correlated to the C13 interval of Bralower et al. (1999) (Fig. 14).

Conclusions

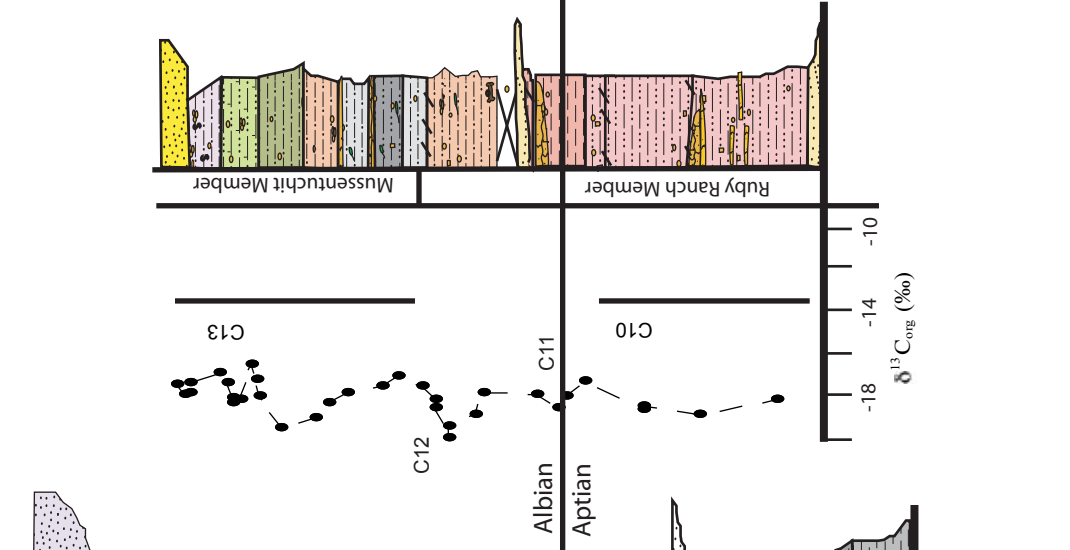
The upper Ruby Ranch and basal Mussentuchit member in the vicinity of the Price River II Quarry (CEU-PR2) in the Price River area, East Central Utah, consist of fluvial sediments, channel fills, palustrine, lacustrine, and paleosols facies, indicating deposition on extensive floodplains. The presence of small carbonate filled ponds, channel calcretes and other micrite and micrite-cemented carbonates, as well

Figure 15. Three point moving average $\delta^{13}\text{C}_{\text{org}}$ and stratigraphic profiles for KU-PR1, KU-PR2 and KU-PR3/4. Carbon excursions C10-C13 are indicated on each profile as correlated with Bralower et al. (1999). Sections are tied-in and hung on the Aptian-Albian boundary (solid black line) set at the first negative shift in excursion C11 (Bralower et al. 1999).

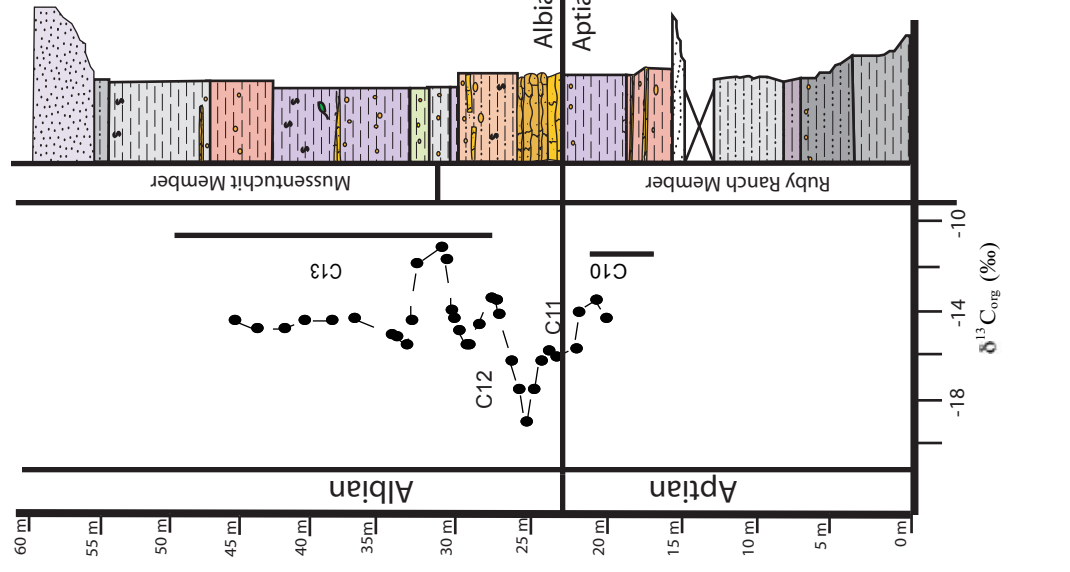
KU-Price River 3/4-Section



KU-Price River 2- Section



KU- Price River 1- Section



as the relatively heavy $\delta^{13}\text{C}_{\text{org}}$ values for KU-PR1, KU-PR2 and KU-PR3/4 sections suggest a seasonal xeric regime, during the development of these floodplain successions.

Organic matter carbon isotope chemostratigraphic profiles ($\delta^{13}\text{C}_{\text{org}}$ for these sections, KU-PR1, 2 and 3/4 are constrained by detrital zircon ages, in the vicinity of CEU-PR2, to have minimum ages in the range of 109 to 116 Ma (Burton et al., 2006). These $\delta^{13}\text{C}_{\text{org}}$ profiles prominent excursions and structure that allow correlation with global $\delta^{13}\text{C}_{\text{org}}$ chemostratigraphy of Bralower et al. (1999). The $\delta^{13}\text{C}_{\text{org}}$ profiles near Price River shows the presence of four distinctive carbon excursions, which are correlated with global carbon isotope curve segments C10 to C13 as defined by Bralower et al., (1999).

Chronostratigraphic control on the global carbon isotope chemostratigraphy places the Aptian-Albian boundary at the step in the negative excursion C11 (Leckie et al., 2002) The correlations of the chemostratigraphic profiles for the Price River sections, in conjunction with current chronostratigraphic data (Burton et al., 2006; Garrison et al., 2007) suggests that the Aptian-Albian boundary is captured by Ruby Ranch Member and makes the upper most Ruby Ranch Member and Mussentuchit Member strictly Albian in age.

References Cited

- Alonso-Zarza, A.M., 2003, Palaeoenvironmental significance of palustrine carbonates and calcretes in the geological record: *Earth-Sciences Reviews*, v. 60, p. 261-298(38).
- Barron, E.J., Fawcett, P.J., Peterson, W.H., Pollard, D., and Thompson, S.L., 1995, A coupled simulation of Late Cretaceous climate and vegetation. AGU spring meeting.
- Barron, E.J., Fawcett, P.J., Pollard, D., Thompson, S., Berger, A., and Valdes, P., 1993, Model Simulations of Cretaceous Climates: The Role of Geography and Carbon Dioxide [and Discussion] *Philosophical Transactions: Biological Sciences; Palaeoclimates and their Modelling with Special Reference to the Mesozoic Era*, v. 341, p. 307-316.
- Barron, E.J., Thompson, S.L., Fawcett, P.J., Peterson, W.H., and Pollard, D., 1995b, A 'simulation' of mid-Cretaceous climate: *Paleoceanography*, v. 10, p. 953-962.
- Bocherens, H., Friis, E.M., Mariotti, A., and Pedersen, K.R., 1993, Carbon isotopic abundances in Mesozoic and Cenozoic fossil plants: Palaeoecological implications *Lethaia*, v. 26, p. 347-358.
- Bralower, T.J., CoBabe, E., Clement, B., Sliter, W.V., Osburn, C.L., and Longoria, J., 1999, The record of global change in Mid-Cretaceous (Barremian-Albian) sections from the Sierra Madre, northeastern Mexico: *Journal of Foraminiferal Research*, v. 29, p. 418-437.
- Brook, E.J., 2005, Atmospheric Science: Tiny Bubbles Tell All: *Science*, v. 310, p. 1285-1287.
- Burton, D., Greenhalgh, B.W., Britt, B.B., Kowalis, B.J., Elliott, W.S.J., and Barrick, R., 2006, New Radiometric Ages from the Cedar Mountain Formation, Utah and the Cloverly Formation, Wyoming: Implications For Contained Dinosaur Faunas, Geological Society of America Annual Meeting: Philadelphia.

- Cerling, T.E., 1991, Carbon Dioxide in the Atmosphere: Evidence from Cenozoic and Mesozoic Paleosols: *American Journal of Science*, v. 291, p. 377-400.
- Cifelli, R.L., Kirkland, J.I., Weil, A., Deino, A.L., and Kowallis, B.J., 1997, High-precision $^{40}\text{Ar}/^{39}\text{Ar}$ geochronology and the advent of North America's Late Cretaceous terrestrial†fauna: *PNAS*, v. 94, p. 11163-11167.
- Cifelli, R.L., Nydam, R.L., Gardner, J.D., Weil, A., Eaton, J.G., Kirkland, J.I., and Madsen, S.K., 1999, Medial Cretaceous vertebrates from the Cedar Mountain Formation, Emery County, Utah; the Mussentuchit local fauna, *in* Gillette David, D., ed., *Vertebrate paleontology in Utah*, Volume 99-1: Miscellaneous Publication - Utah Geological Survey: Salt Lake City, UT, United States, Utah Geological Survey, p. 219-242.
- Currie, B.S., 1998, Upper Jurassic-Lower Cretaceous Morrison and Cedar Mountain formations, NE Utah-NW Colorado; relationships between nonmarine deposition and early Cordilleran foreland-basin development: *Journal of Sedimentary Research*, v. 68, p. 632-652.
- , 2002, Structural configuration of the Early Cretaceous Cordilleran foreland-basin system and Sevier thrust belt, Utah and Colorado: *Journal of Geology*, v. 110, p. 697-718.
- DeCelles, P.G., 2004, Late Jurassic to Eocene evolution of the Cordilleran thrust belt and foreland system, western U.S.A: *American Journal of Science*, v. 304, p. 105-168.
- DeCelles, P.G., and Currie, B.S., 1996, Long-term sediment accumulation in the Middle Jurassic-early Eocene Cordilleran retroarc foreland-basin system: *Geology*, v. 24, p. 591-594.
- Demko, T.M., Currie, B.S., and Nicoll, K.A., 2004, Regional paleoclimatic and stratigraphic implications of paleosols and fluvial/overbank architecture in the Morrison Formation(Upper Jurassic), Western Interior, USA: *Sedimentary Geology*, v. 167, p. 115-135.

- Erbacher, J., Huber, B.T., Norris, R.D., and Markey, M., 2001, Increased thermohaline stratification as a possible cause for an ocean anoxic event in the Cretaceous period: *Nature*, v. 409, p. 325-327.
- Farquhar, G.D., Ehleringer, J.R., and Hubick, K.T., 1989, Carbon Isotope Discrimination and Photosynthesis: *Annual Review of Plant Physiology and Plant Molecular Biology*, v. 40, p. 503-537.
- Garrison, J.R.J., Donald Brinkman, Douglas J. Nichol, Paul Layerd, Burgee, D., and Thayne, D., 2007, A multidisciplinary study of the Lower Cretaceous Cedar Mountain Formation, Mussentuchit Wash, Utah: a determination of the paleoenvironment and paleoecology of the Eolambia caroljonesa dinosaur quarry: *Cretaceous Research*, v. 28, p. 461-494.
- Grocke, D.R., Hesselbo, S.P., and Jenkyns, H.C., 1999, Carbon-isotope composition of Lower Cretaceous fossil wood: Ocean-atmosphere chemistry and relation to sea-level change: *Geology*, v. 27, p. 155-158.
- Hallam, A., 1985, A review of Mesozoic climates: *Journal - Geological Society (London)*, v. 142, p. 433-445.
- , 1986, Role of climate in affecting late Jurassic and early Cretaceous sedimentation in the North Atlantic, *in* Summerhayes, C.P., ed., *North Atlantic palaeoceanography: Geological Society Special Publication*, 21, Blackwell Scientific, p. 277-281.
- Hasiotis, S.T., 2002, Continental trace fossils: *SEPM Short Course Notes 51*, Society for Sedimentary Geology, Tulsa, OK, 132p.
- Heimhofer, U., Hochuli, P.A., Burla, S., Dinis, J.M.L., and Weissert, H., 2005, Timing of Early Cretaceous angiosperm diversification and possible links to major paleoenvironmental change: *Geology*, v. 33, p. 141-144.
- Jahren, A.H., Arens, N.C., Sarmiento, G., Guerrero, J., and Amundson, R., 2001, Terrestrial record of methane hydrate dissociation in the Early Cretaceous: *Geology*, v. 29, p. 159-162.

- Jenkyns, H., 2000, Cretaceous oceanic anoxic events and carbon isotopes: Implications for global change: *Fossils*, v. 68, p. 20-21.
- Jenkyns, H., C., 2003, Evidence for rapid climate change in the Mesozoic-Palaeogene greenhouse world.; Abrupt climate change; evidence, mechanisms and implications; papers of a discussion meeting: *Philosophical Transactions of the Royal Society A: Mathematical, Physical and Engineering Sciences*, v. 361, p. 1885-1916.
- Jenkyns, H.C., 1980, Cretaceous anoxic events: from continents to oceans: *Journal of the Geological Society*, v. 137, p. 171-188.
- Kirkland, J.I., 2005, Utah's Newly Recognized Dinosaur Record from the Early Cretaceous Cedar Mountain Formation: *Utah Geological Survey, Survey Notes*, v. 37, p. 1-5.
- Kirkland, J.I., Cifelli, R.L., Britt, B.B., Burge, D.L., DeCourten, F.L., Eaton, J.G., and Parrish, J.M., 1999, Distribution of vertebrate faunas in the Cedar Mountain Formation, east-central Utah, *in* Gillette David, D., ed., *Vertebrate paleontology in Utah.*, Volume 99-1: Miscellaneous Publication - Utah Geological Survey: Salt Lake City, UT, United States, Utah Geological Survey, p. 201-217.
- Kraus, M.J., 1987, Integration of channel and floodplain suites; II, Vertical relations of alluvial Paleosols: *Journal of Sedimentary Research*, v. 57, p. 602-612.
- Larson, R.L., and Erba, E., 1999, Onset of the Mid-Cretaceous greenhouse in the Barremian-Aptian; igneous events and the biological, sedimentary, and geochemical responses: *Paleoceanography*, v. 14, p. 663-678.
- Leckie, R.M., Bralower, T.J., and Cashman, R., 2002, Oceanic anoxic events and plankton evolution; biotic response to tectonic forcing during the Mid-Cretaceous: *Paleoceanography*, v. 17.
- Leng, M., Lamb, A.L., Heaton, T.H.E., Marshall, J.D., Wolfe, B.B., Jones, M.D., and Holmes, J.A., 2006, Isotopes in Lake Sediments, *in* Leng, M.J., ed., *Isotopes*

- in Palaeoenvironmental Research, Volume 10, Springer Netherlands, p. 147-184.
- Lockley, M.G., White, D., Kirkland, J., and Santucci, V., 2004, Dinosaur tracks from the Cedar Mountain Formation (Lower Cretaceous), Arches National Park, Utah: *Ichnos*, v. 11, p. 285-293.
- McLaren, S., 2004, Characteristics, evolution and distribution of Quaternary channel calcretes, southern Jordan: *Earth Surface Processes and Landforms*, v. 29, p. 1487-1507.
- Midwood, A.J., and Boutton, T.W., 1998, Soil carbonate decomposition by acid has little effect on delta¹³C of organic matter: *Soil Biology & Biochemistry*, v. 30, p. 1301-1307.
- Nash, D.J., and Smith, R.F., 1998, Multiple calcrete profiles in the Tabernas Basin, southeast Spain: their origins and geomorphic implications: *Earth Surface Processes and Landforms*, v. 23, p. 1009-1029.
- Nelson, M.E., and Crooks, D.M., 1987, Stratigraphy and Paleontology of the Cedar Mountain Formation (Lower Cretaceous), Eastern Emery County Utah, *in* Averett, W.R., ed., *Dinosaur Triangle Paleontological Field Trip: Grand Junction, Colorado*, Museum of Western Colorado, p. 55-63.
- Petit, J.R., Jouzel, J., Raynaud, D., Barkov, N.I., Barnola, J.M., Basile, I., Bender, M., Chappellaz, J., Davis, M., Delaygue, G., Delmotte, M., Kotlyakov, V.M., Legrand, M., Lipenkov, V.Y., Lorius, C., Pepin, L., Ritz, C., Saltzman, E., and Stievenard, M., 1999, Climate and atmospheric history of the past 420,000 years from the Vostok ice core, *Antarctica: Nature*, v. 399, p. 429-436.
- Poulsen, C.J., Barron, E.J., Arthur, M.A., and Peterson, W.H., 2001, Response of the mid-Cretaceous global oceanic circulation to tectonic and CO₂ forcings: *Paleoceanography*, v. 16, p. 576-592.

- Robinson, S.A., and Hesselbo, S.P., 2004, Fossil-wood carbon-isotope stratigraphy of the non-marine Wealden Group (Lower Cretaceous, southern England): *Journal of the Geological Society*, v. 161, p. 133-145.
- Sanz, M.E., Alonso Zarza, A.M., and Calvo, J.P., 1995, Carbonate pond deposits related to semi-arid alluvial systems: examples from the Tertiary Madrid Basin, Spain: *Sedimentology*, v. 42, p. 437.
- Sereno, P.C., 1997, The origin and evolution of dinosaurs: *Annual Review of Earth and Planetary Sciences*, v. 25, p. 435-489.
- Smith, B.N., and Epstein, S., 1971, Two Categories of $^{13}\text{C}/^{12}\text{C}$ Ratios for Higher Plants: *Plant Physiology*, v. 47, p. 380-384.
- Spicer, R.A., and Corfield, R.M., 1992, A review of terrestrial and marine climates in the Cretaceous with implications for modelling the "Greenhouse Earth": *Geological Magazine*, v. 129, p. 169-180.
- Sprinkel, D.A., Weiss, M.P., Fleming, R.W., and Waanders, G.L., 1999, Redefining the Lower Cretaceous stratigraphy within the central Utah foreland basin, Utah Geological Survey: Special Study 97: Salt Lake City, Utah, Utah Department of Natural Resources.
- Stokes, W.M.L., 1952, Lower Cretaceous in Colorado Plateau: *Bulletin of the American Association of Petroleum Geologists*, v. 36, p. 1766-1776.
- Tieszen, L.L., 1991, Natural variations in the carbon isotope values of plants: implications for archaeology, ecology, : *Journal of Archaeological Science*, v. 18, p. 227-248.
- Ufnar, D.F., Brenner, R.L., Witzke, B.J., Gonzalez, L.A., and Ludvigson, G.A., 2002, The mid-cretaceous water bearer: Isotope mass balance quantification of the Albian hydrologic cycle: *Palaeogeography, Palaeoclimatology, Palaeoecology*, v. 188, p. 51-71.
- White, T., S., Witzke, B., J., and Ludvigson, G., A., 2001, Middle Cretaceous greenhouse hydrologic cycle of North America: *Geology*, v. 29, p. 363-366.

Yingling, V.L., and Heller, P.L., 1992, Timing and record of foreland sedimentation during the initiation of the Sevier orogenic belt in central Utah: Basin Research, v. 4, p. 279-290.

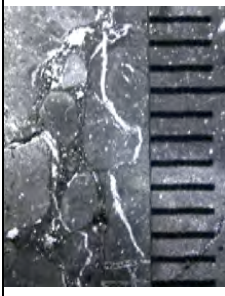
Appendix A: Field Notes KU- Price River 1 Section

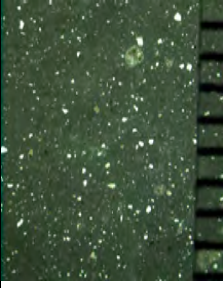
For detailed site location, information including longitude and latitude of sites or to visit site locations in this study, please contact the, State Paleontologist, Utah Geological Survey , 1594 West North Temple, Suite 3110, P.O. Box 146100 Salt Lake City, UT 84114-6100; TEL (801) 537-3307 FAX (801) 537-3400

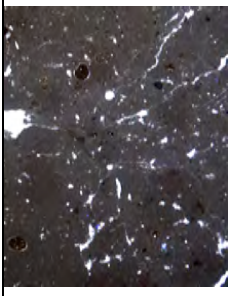
Sample #	Depth bed(m)	Depth total(m)	Color	Lithology	Description	Notes/Thin Section Images
KU-PR1-1	0.45	57.94	White→ Red/Purple	Sandy Mudstone	Red and purple coloration occurs as mottles, lots of iron oxide.	
KU-PR1-2	0.94	57.49	White→ Gray	Sandy Mudstone	Blocky unit, some lamination (0.4m) in a dark gray color fine grained.	
KU-PR1-3	1.45	56.55	Gray	Mudstone	Mottled coloration, lots of iron oxide staining. Some slickensides, weakly vertic ped structures, very fine clay/silt contrasting overlying coarser units.	
KU-PR1-4	0.73	55.1	Gray→ Red	Mudstone	Red coloration occurs as mottles. Ped's appear vertic. Evidence of bioturbation, Slickensides.	
No Sample	2.30	54.37	Gray	Mudstone	Highly weathered mudstone not dissimilar to overlying mudstone.	
KU-PR1-5	1.80	52.07	Gray	Mudstone	Highly fractured compacted massive structureless mudstone. Tectonics ?	

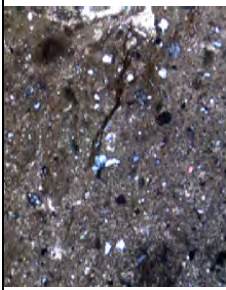
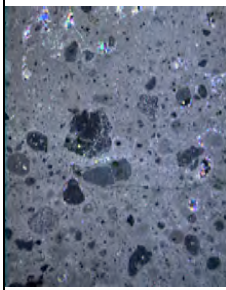
Sample #	Depth bed(m)	Depth total(m)	Color	Lithology	Description	Notes/Thin Section Images
KU-PR1-6	2.04	50.27	Gray	Carbonate bearing Mudstone	The base of the unit is punctuated a thin carbonate unit (0.1). Above this unit is a muddy unit with carbonate nodules entrained it into it (2-20cm d). Gradation from nodules to indurated calcarete bed. Mudstone is very effervescent, nodules become larger and larger towards the top of the unit. Sharp slope break were nodules occur indicating weathering of slope but no weathering of carbonate bed. Carbonate bed is only 0.42m thick.	
KU-PR1-7	0.67	48.23	Red → White/Gray	Mudstone	Same as PR1-8	
KU-PR1-8	1.20	47.56	Red → White/Gray	Mudstone	Abrupt contact with overlying unit. White/gray mottles/lenses no effervescent. Breaks in to ABK and some small SBK when blocks are pulled out.	

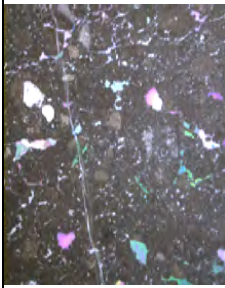
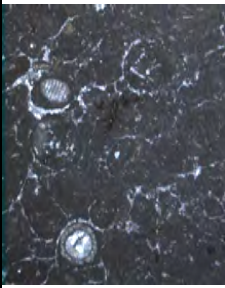

Sample #	Depth bed(m)	Depth total(m)	Color	Lithology	Description	Notes/Thin Section Images
KU-PR1-9	0.30	46.36	Red	Mudstone	Some small carbonate nodules (0.2-2cm d) entrained in the muddy matrix. Also thin 30cm thick calcarete bed in places.	
KU-PR1-10	1.24	46.06	Red→Gray	Mudstone	Some small gray lenses of material. No effervescences. Also some dark fragments, organic matter?. Transitions in to unit above abruptly.	
KU-PR1-11	1.41	44.82	Purple	Mudstone	Contact is abrupt. Unit is darker than overlying units with no gray mottling. No effervescent. High shrink swell when in contact with water. Stacked angular blocky units.	
KU-PR1-12	1.85	43.41	Purple→Gray	Mudstone	More clay in this unit than overlying units, but also more weathered, with some gray mottling.	
KU-PR1-13	1.32	41.56	Purple→Gray/Green	Mudstone	Very soft, clay rich unit black and green coloration is in mottles, iron oxide staining. Very weak effervescent. Slickensides and some clay skins.	

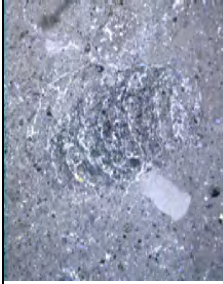

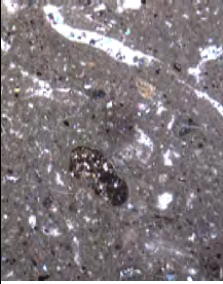

Sample #	Depth bed(m)	Depth total(m)	Color	Lithology	Description	Notes/Thin Section Images
KU-PR1-14	1.95	40.24	Purple→Gray	Mudstone	Gray occurs as mottles, with some iron oxide staining no other sedimentary features.	
KU-PR1-15	1.41	38.29	Purple→Gray	Mudstone	Gray occurs as mottles. No major lithologic change. OM rich material concentrated in a discontinuous bed directly above lenticular carbonate, 10-20cm thick.	
No sample	0.1	36.88	Red→green mottles	Carbonate bearing mudstone	Lenticular carbonate unit, n red-green mottled mudstone the unit is not continuous and pinches out. Bed corresponds with slope break	Difficult to sample on a steep slope.
KU-PR1-16	1.33	36.78	Red→ Gray/Green mottles	Carbonate nodule bearing mudstone	Again gray/green mottling, in red matrix small 0.1-1cm carbonate nodules, ped's are angular blocky.	
KU-PR1-17	1.03	35.45	Purple/Red →Gray mottles	Mudstone	No effervescences, very friable unit. Likely deformed by tectonics. Gray occurs as mottling.	
KU-PR1-18	0.36	34.42	Purple/Red →Gray mottles	Mudstone	Carbonate nodules, ranging in size from 2-20cm in diameter. Has abrupt lower and upper boundaries with surrounding units.	


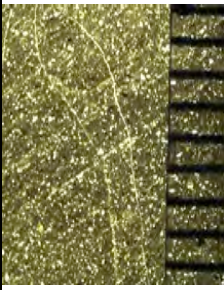
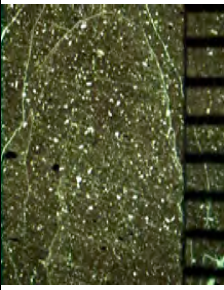
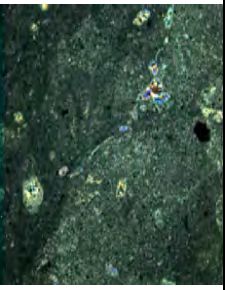
Sample #	Depth bed(m)	Depth total(m)	Color	Lithology	Description	Notes/Thin Section Images
KU-PR1-19	0.73	34.06	Purple/Red→Gray mottles	Mudstone	Same as P1-18 but nodules are much smaller at the base, grading in to much larger nodules at the top.	
KU-PR1-20	0.38	33.33	Gray/Green	Mudstone	Carbonate nodules present very clay rich, compared to overlying unit.	
KU-PR1-21	0.27	32.95	Gray/Green	Mudstone	No carbonate nodules, no effervescences.	
KU-PR1-22	0.42	32.68	Dark gray→Gray	Mudstone	Few carbonate nodules here. No other structures. Some gray mottling.	
KU-PR1-23	0.29	32.26	Gray→dark gray	Mudstone	Fewer small carbonate nodules than overlying horizon.	
KU-PR1-24	0.27	31.97	Gray→dark gray	Silty Mudstone	Higher silt concentration than overlying units, mottling of colors. Few small carbonate nodules. 0.1 to 2cm d nodules	
KU-PR1-25	0.35	31.7	Gray→dark gray	Silty Mudstone	Similar to overlying unit with fewer carbonate nodules.	
KU-PR1-26	0.54	31.35	Gray→Purple	Silty Mudstone	Same as above	


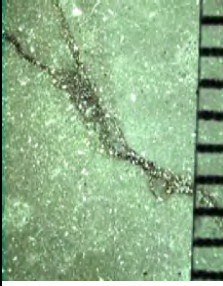
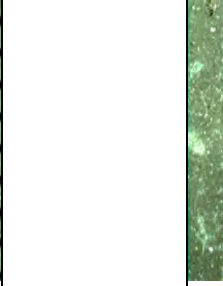
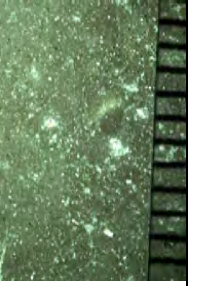
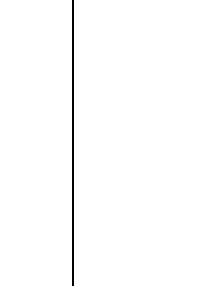
Sample #	Depth bed(m)	Depth total(m)	Color	Lithology	Description	Notes/Thin Section Images
KU-PR1-27	0.47	30.81	Red→Gray	Carbonate nodule bearing and indurated mudstone	Highly mottled mudstone, lots of large carbonate nodules. No major sedimentary features. Nodules form lenticular beds where coalesced and cemented. Only occurs at the top of the unit. Nodules are free floating towards to the base of the unit ref. PR1-28.	
KU-PR1-28	0.25	30.34	Red	Carbonate nodule bearing mudstone	Large carbonate nodule collected here. Matrix same as PR1-27	
KU-PR1-29	0.58	30.09	Red→Gray	Mudstone	Very mottled, with some black clasts entrained (organic material?). May have some thickly laminated bedding planes.	
KU-PR1-30	0.90	29.51	Red/Orange→Gray	Carbonate nodule bearing mudstone	Large carbonate concretions occur at the top of this bed, matrix is somewhat lighter than overlying red unit. With less gray mottling. 1-10 to 20cm (d) top . 5% base 25% top.	

Sample #	Depth bed(m)	Depth total(m)	Color	Lithology	Description	Notes/Thin Section Images
KU-PR1-31	0.50	28.61	Purple/Red → Gray	Mudstone	Some slickensides, clay skins between bedding plains or peds. Color becomes lighter red grading in to purple unit. Only Slightly effervescent. Image is cross polarized.	
KU-PR1-32	0.50	28.11	Red→Black	Mudstone	Some black mottling, no effervescences no carbonate nodules, angular block peds.	
KU-PR1-33	0.50	27.61	Red/Orange → Gray	Mudstone	Gray/dark gray mottles/lenses, some small slickensides, and clay skins. Angular blocky peds. Very effervescent.	
KU-PR1-34	0.36	27.11	Red/Orange → Gray	Mudstone	Same as PR1-33. But much more orange at base.	
KU-PR1-35	0.50	26.75	Orange/White	Indurated Carbonate	Orange and white mottled. Calcrete is bedded, blocky units. Forms a slope break/well indurated thick.	
KU-PR1-36	0.50	26.25	Orange/White	Indurated Carbonate	Same as PR1-35. Image is cross polarized	

Sample #	Depth bed(m)	Depth total(m)	Color	Lithology	Description	Notes/Thin Section Images
KU-PR1-37	0.50	25.75	Orange/White	Indurated Carbonate	Image is cross-polarized.	
KU-PR1-38	0.50	25.25	Orange/White	Indurated Carbonate		
KU-PR1-39	0.50	24.75	Orange/White	Indurated Carbonate		
KU-PR1-40	0.50	24.25	Orange/White	Indurated Carbonate		

Sample #	Depth bed(m)	Depth total(m)	Color	Lithology	Description	Notes/Thin Section Images
KU-PR1-41	0.61	23.75	Orange/White	Indurated Carbonate	Image is cross-polarized.	
KU-PR1-42	0.65	23.14	Purple	Carbonate nodule bearing Mudstone	Gradational contact with carbonate rich orange unit. Bed still contains carbonate nodules but much small and not as indurated.	
KU-PR1-43	0.26	22.49	Purple	Mudstone	No carbonate nodules, clay rich. Effervescent	
KU-PR1-44	0.45	22.23	Purple	Mudstone	Similar to PR1-43	

Sample #	Depth bed(m)	Depth total(m)	Color	Lithology	Description	Notes/Thin Section Images
KU-PR1-45	1.07	21.78	Purple	Clay Rich Mudstone	Very nodular in appearance. Friable as unit gets less indurated/clay rich.	
KU-PR1-46	0.64	20.71	Purple	Mudstone	Very friable. No other sedimentary structures no cf.	
KU-PR1-47	0.35	20.07	Purple	Mudstone	Very friable, slight effervescent.	
KU-PR1-48	0.30	19.72	Purple/Red	Indurated Carbonate	New Calcrete bed forms a ledge, blocky, intermixed calcareous nodules and carbonate cemented mudstone beds.	
KU-PR1-49	0.63	19.42	Purple/Red	Carbonate nodule bearing mudstone	Carbonate nodules in muddy matrix, very clay rich.	



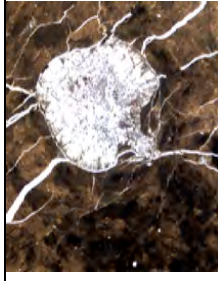
Sample #	Depth bed(m)	Depth total(m)	Color	Lithology	Description	Notes/Thin Section Images
KU-PR1-50	0.60	18.79	Purple/Red	Carbonate nodule bearing mudstone	Mudstone/Clay becomes more fragmented; carbonate nodules are scattered but still large.	
KU-PR1-51	0.33	18.19	Purple/Red	Cemented indurated horizon	Carbonated becomes more indurated blocky. Welded, nodules are not floating in a muddy matrix, but form a cohesive bed. Muddy rind around all nodules.	
KU-PR1-52	0.25	17.86	Purple/Red	Carbonate nodule bearing mudstone		
KU-PR1-53	0.62	17.61	Purple/Red	Carbonate nodule bearing mudstone	Nodules no longer form welded horizon. Large nodules in muddy matrix. Much less than in upper units.	
KU-PR1-54	0.75	16.99	Purple/Red	Carbonate nodule bearing mudstone	Less nodules, and an increase in the amount of matrix.	

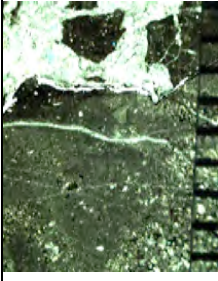
Sample #	Depth bed(m)	Depth total(m)	Color	Lithology	Description	Notes/Thin Section Images
KU-PR1-55	0.96	16.24	White/Yellow	Sandstone	Cross bedded, fining upward, medium-coarse grained sand . 1-2 cm of mud are visible.	
Cover	1.40	15.28		Soil/Colluvium		
KU-PR1-1A	2.18	13.88	Gray	Mudstone	Lots of modern roots, secondary redox features. SBK.	
KU-PR1-2A	3.10	11.7	Gray/purple	Clay rich mudstone	Higher clay content than overlying unit.	
KU-PR1-3A	0.86	8.6	Purple/Brown	Clay rich mudstone	High clay content altered by modern roots.	
KU-PR1-4A	2.17	7.74	Green/Gray	Clay rich mudstone	Shrink swell clay, some small carbonate nodules, ABK ped structure.	
KU-PR1-5A	1.26	5.57	Dark Gray	Clay rich mudstone	Same as PR1-4A	
KU-PR1-6A	1.16	4.31	Gray/Purple	Mudstone	Some evidence of bioturbation and dark, plant fragments.	
KU-PR1-7A	0.98	3.15	Gray/Purple	Mudstone	Same as PR1-6A	
KU-PR1-8A	2.17	0→2.17	Gray/Purple	Mudstone	Same as PR1-6A	

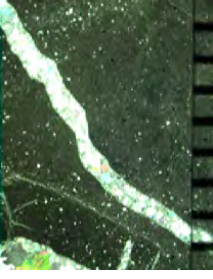
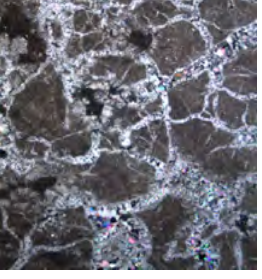
Appendix B: Field notes for KU-Price River 2 Section –



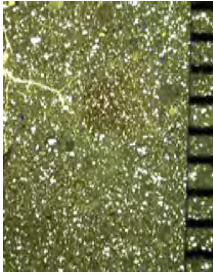
Utah Geological Survey Ascension Number EM 372

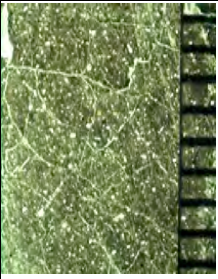
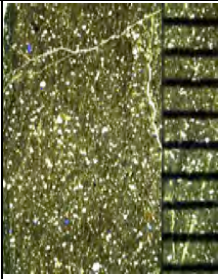
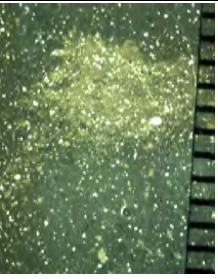
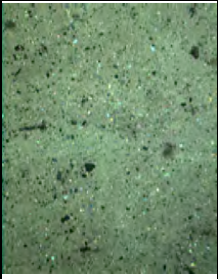
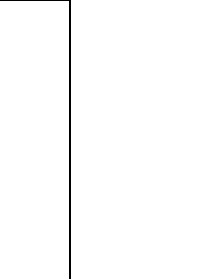

*For detailed site location, information including longitude and latitude of sites or to visit site locations in this study, please contact the, State Paleontologist, Utah Geological Survey , 1594 West North Temple, Suite 3110, P.O. Box 146100
Salt Lake City, UT 84114-6100; TEL (801) 537-3307 FAX (801) 537-3400*


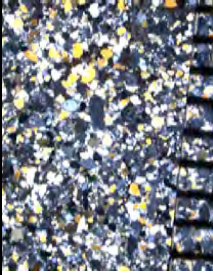

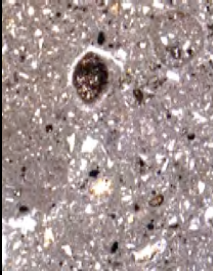
Sample #	Depth bed(m)	Depth total(m)	Color	Lithology	Description	Thin Section Images
KU-PR2-1	0.40	41.35	Red → Grey	Mudstone	Coalesced carbonate nodules weather out and appear in the mud matrix, variegated color. Some slickensides. Image is cross-polarized.	
KU-PR2-2	0.50	40.95	Red → Grey/Green	Mudstone	Slickensides no carbonate nodules, some angular blocky and sub-angular blocky ped structures. Ped's are also stained with iron oxide on outside. Maybe some organic matter.	
KU-PR2-3	0.48	40.45	Red → Grey/Green	Mudstone		
KU-PR2-4	0.30	39.97	Red → Grey/White	Mudstone	Abrupt contact with overlying greener unit. Very effervescent unit, lots of small 0.1-5cm coalesced nodules. Beds appear disrupted; ped's appear to be ABK/SBK.	
KU-PR2-5	1.00	39.67	Grey/Green → Red	Mudstone	Abrupt contact with overlying redder unit. Small carbonate cemented bed, very effervescent. Small 0.1-5cm coalesced carbonate nodules.	


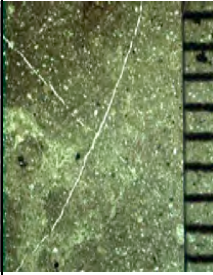
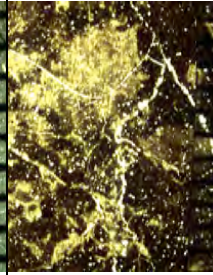

Sample #	Depth bed(m)	Depth total(m)	Color	Lithology	Description	Thin Section Images
KU-PR2-6	0.97	38.67	Grey/Green → Red	Mudstone		
KU-PR2-7	0.40	37.7	Grey/Green → Red	Mud-Claystone	Clay skins present, less red then overlying unit, some black fragments (organic matter?). Again very effervescent, with 1-3cm carbonate nodules.	
KU-PR2-8	0.37	37.3	Grey/Green → Red	Mud-Claystone		
KU-PR2-9	0.54	36.93	Green→ Yellow	Mudstone	Abrupt contact with overlying red/grey units. ABK/SBK ped structures.	
KU-PR2-10	0.66	36.39	Green→ Red/Yellow	Mudstone	Gradational contact. Interfingers with underlying thin carbonate bed.	
KU-PR2-11	0.49	35.73	Red→Green	Calcareous unit	Sub-spherical blocks mostly 20cm in diameter. Violent effervescence. Abrupt contact with underlying unit. Undulating top.	
KU-PR2-12	0.17	35.24	Red→Green	Mudstone	Abrupt contact with overlying unit. No effervescence. Very friable. Abrupt contact with underlying and overlying unit.	

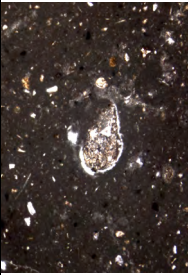
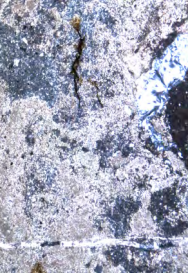

Sample #	Depth bed(m)	Depth total(m)	Color	Lithology	Description	Thin Section Images
KU-PR2-13	1.33	35.07	Green→ Grey	Mudstone	Clay rich unit, ABK/SBK peds. Mottled color, black fragments (organic matter?). No effervescences.	
KU-PR2-14	0.62	33.74	Grey→ White	Sandy Mudstone	Mudstone with some upper fine to lower medium sand sized particles. Effervescent, carbonate cementation. Darker fragments, organic matter? Coal?	
KU-PR2-15	1.67	33.12	Grey→ White	Sandy Mudstone		
KU-PR2-16	0.79	31.45	Grey→ White	Indurated Carbonate	Quarry; top of quarry unit, very indurated with iron oxide staining on some block faces.	
KU-PR2-17	1.06	30.66	Red→Grey	Fossil-bearing Mudstone	Quarry; dinosaurian are mostly brachiosaur, though some gastropods have also been found. Bones are typically coated in carbonate nodules. Some evidence of iron oxide on block faces from the quarry. Very effervescent, SBK/ABK Peds. Organic rich, layer. Bones appear to have orientation. Image is cross polarized.	

Sample #	Depth bed(m)	Depth total(m)	Color	Lithology	Description	Thin Section Images
KU-PR2-18	0.20	29.6	Dark Grey	Sandy Mudstone	Organic rich sandier than overlying units, layered bedding. Very effervescent,	
KU-PR2-19	0.58	29.4	Grey	Carbonate cemented Mudstone	Not as organic rich as overlying unit, some iron oxide mottling, blocky units. May onlap. Very effervescent.	
KU-PR2-20A	1.7	28.82	Grey→ White/ Red	Fossil-Bearing Mudstone	Large rip up clasts of dark grey mudstone, organic matter rich, very little effervescences at top of unit. Very friable, not well cemented. ABK and SBK peds or blocks. Some very red nodules very friable. Has a similar reddish color as the main quarry. Medium-thickly bedded (?). Some bones, few. Base of unit has an abrupt contact with underlying limey mudstone, more brachiosaur remains in this lower unit. Effervescent with some large carbonate nodules, amongst the bones. Abrupt contact with lower limestone unit.	

Sample #	Depth bed(m)	Depth total(m)	Color	Lithology	Description	Thin Section Images
KU-PR2-20B	1.07	27.12	Grey→ White mottled	Limey Mudstone	Very indurated, and clay rich with organic matter fragments.	
KU-PR2-21	1.55	26.05	Grey→ White mottled	Sandy Mudstone	Laminated mudstone, friable, with abrupt contact, with lower red unit. Some grey/purple mottling, black fragments (organic matter?). Grades In to redder unit, some rip up clasts near base. Also some sand.	
KU-PR2-22	0.76	24.5	Red→ Brown	Mudstone	Blocky peds. Massive. No effervescence	
KU-PR2-23	0.97	23.74	Red→ Yellow	Carbonate nodule rich Mudstone	Thin 0.25m carbonate unit at top of this mudstone unit, as you move down the bed less indurated carbonate and more carbonate nodules, eventually grading into mudstone with few nodules (see sample PR2-24).	
KU-PR2-24	1.17	22.77	Red→ Yellow	Mudstone	Few carbonate nodules, yellow mottles in the red matrix.	
KU-PR2-25	0.50	21.6	Red	Mudstone	Some small sand lenses 0.5cm wide in red muddy matrix not predominant.	

Sample #	Depth bed(m)	Depth total(m)	Color	Lithology	Description	Thin Section Images
KU-PR2-26	0.50	21.1	Red	Mudstone	No obvious bedding or sedimentary features, very weathered. Slope deposit	
KU-PR2-27	3.50	20.6	Red	Soil (modern)	Cover (Grab Sample) Red Soil	
KU-PR2-28C	1.50	17.1	White → Yel low	Poorly sorted sandstone	Poorly sorted channel sandstone, cuts in to underlying mudstone/carbonate unit. Cross bedded. Image is cross-polarized.	
KU-PR2-28B	0.50	15.6	Red	Mudstone	Blocky, clay rich. No bedding plains or other sedimentological features.	
KU-PR2-28A	1.20	15.1	Red	Indurated Carbonate	Calcrete bed massive contorted, many 5-15cm nodules. Mainly purple/red matrix coated. Nodules are yellow internally. Nodules occur in massive carbonate indurated horizon. Image is cross polarized.	
KU-PR2-29C	1.6	13.9	Dark Red	Silty Mudstone	Compacted silty mudstone, massive. Abrupt contact with upper and lower unit.	


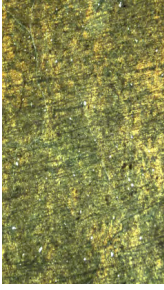
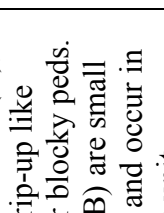
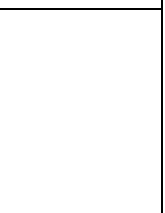
Sample #	Depth bed(m)	Depth total(m)	Color	Lithology	Description	Thin Section Images
KU-PR2-29B	0.70	12.3	Red	Carbonate nodule bearing Mudstone	Mudstone with large upright / vertic carbonate nodules at base. Mudstone similar to unit above massive calcrete bed.	
KU-PR2-29A	1.68	11.6	Red/Purple	Mudstone	Blocky ped faces. ABK. Carbonate nodules disappear no other sedimentary structures.	
KU-PR2-30	2.00	10.12	Red/Purple	Carbonate nodule bearing Mudstone	Muddy matrix with large columnar nodules. Vertically stacked, coalesced nodules. Grades up from a calcrete bed below.	
KU-PR2-31	1.60	8.12	Red/Purple	Indurated Carbonate	Coalesced carbonate nodules. Abrupt contact with basal mudstone. Interfingers with mudstone at the edges of the bed where it pinches out. Grades in to more stacked carbonate nodules that are not in a continuous bed.	


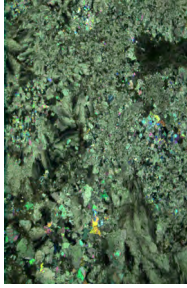
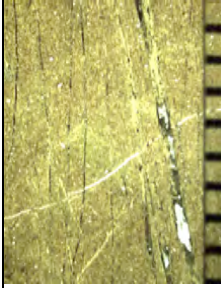
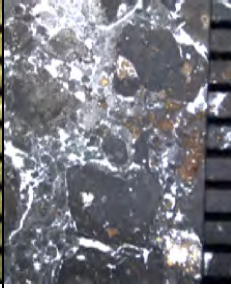
Sample #	Depth bed(m)	Depth total(m)	Color	Lithology	Description	Thin Section Images
KU-PR2-32	0.40	6.52	Red/Purple	Calcrete Nodule Rich Mudstone	Large carbonate nodules diameter 10-20cm, entrained in muddy matrix. Pinches out to the sides. Appears layered.	
KU-PR2-33	3.66	6.12	Red/Purple	Carbonate Nodule Rich mudstone	Carbonate nodules form lenticular beds, that are undulating and contorted very blocky carbonate units that interfinger with mudstone.	
KU-PR2-34	0.50	2.46	Red/Purple	Mudstone	Muddy Matrix with entrained carbonate nodules grading into upper carbonate nodule rich unit.	
KU-PR2-35	0.50	1.96	Red/Purple	Mudstone	Very friable mudstone, breaks in to angular blocky ped's but is likely not primary possibly due to tectonic deformation, creating brittle mudstone. See PR2-35	
KU-PR2-36	0.50	1.46	Red/Purple	Mudstone	See PR2-35	
KU-PR2-37	0.96	0.96	Red/Purple	Mudstone	See PR2-35	
No Sample			White→ Yellow	Cross – laminated Sandstone	Fining upward sandstone with cross laminations. Poorly sorted. Abrupt contact with overlying mudstone.	


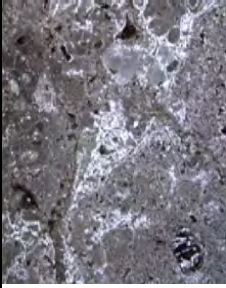
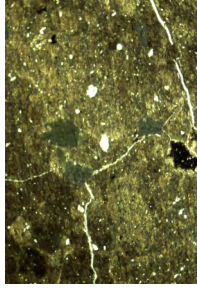
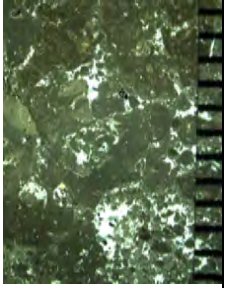
Appendix C: Field notes for KU-Price River 3/4 Section

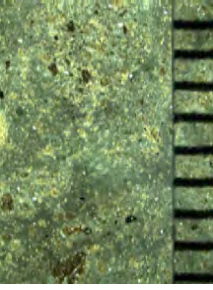
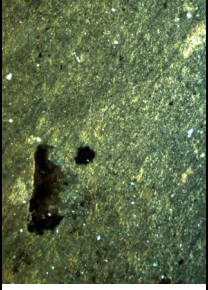
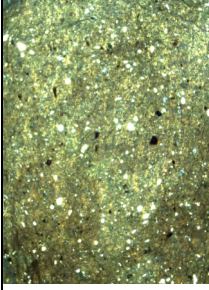
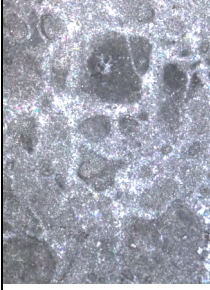
For detailed site location, information including longitude and latitude of sites or to visit site locations in this study, please contact the State Paleontologist, Utah Geological Survey, 1594 West North Temple, Suite 3110, P.O. Box 146100 Salt Lake City, UT 84114-6100; TEL (801) 537-3307 FAX (801) 537-3400

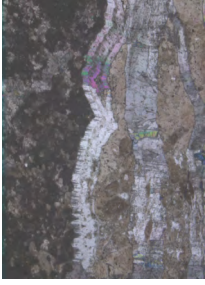
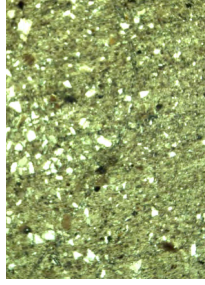
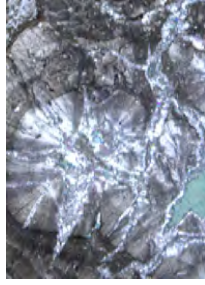
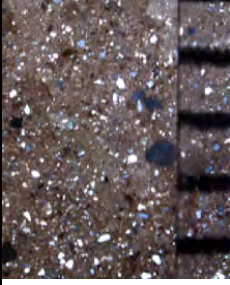
Sample #	Depth bed(m)	Depth total(m)	Color	Lithology	Description	Notes/Thin Section Image
KU-PR3-1	0.97	49.35	Tan	Sandstone	Carbonate cemented sandstone, well sorted, fining upward, upper-fine to medium sized sand. Some quartz veins running through sandstone. Cross-bedded.	
KU-PR3-2	0.7	48.38	Tan	Conglomerate	Cobble, pebble, and gravel sized clasts. Effervescent matrix. Matrix is upper fine sand. Clasts are 60% limestone/ carbonate and 40% other types of rocks. Poorly sorted, no grading.	
KU-PR3-3	0.61	47.68	Tan	Conglomerate	Base of conglomerate, coarsening upward, same composition as PR3-2. Pebble lag at very base unconformably resting on underlying Claystone.	
KU-PR3-4	0.89	47.07	Yellow→ Grey	Claystone	Highly weathered abrupt contact with conglomerate. High clay content very friable	
KU-PR3-5	0.91	46.18	Grey→ Black	Mudstone	Mottled grey coloration, black flecks (original color?) visible in rocks. No effervescences, some slickensides.	
KU-PR3-6	0.66	45.27	Grey	Mudstone	Ref. PR3-5	

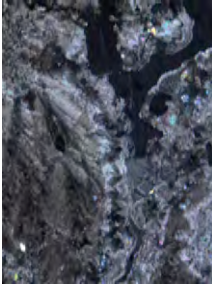
Sample #	Depth bed(m)	Depth total(m)	Color	Lithology	Description	Notes/Thin Section Image
KU-PR3-7	0.65	44.61	Grey → Light grey	Claystone	Mottled grey coloration, high shrink swell, and slight effervescence. Small black rip-up like clasts. Angular blocky peds.	
KU-PR3-8	0.61	43.96	Grey	Claystone	Angular blocky peds, no effervescence high shrink swells.	
KU-PR3-9A/B	0.72	43.35	Grey → Dark grey	Mudstone	No effervescences in matrix (A), some clay enriched rip-up like clasts. Small angular blocky peds. Carbonate nodules (B) are small 0.1-2cm in diameter and occur in the upper 2cm of the unit.	A.  B. 

Sample #	Depth bed(m)	Depth total(m)	Color	Lithology	Description	Notes/Thin Section Image
KU-PR3-10A/B	0.58	42.63	Dark Grey	Mudstone	No effervescences in matrix (A), some small 0.5-3cm-diameter carbonate nodules (B), interrupt bedding planes. Occur between beds. Beds are angular to sub-angular blocky. Image (B) is cross polarized.	A.  B. 
KU-PR3-11	0.6	42.05	Grey	Mudstone	Very friable, no effervescences. Sub-angular blocky beds.	
KU-PR3-12	0.54	41.45	Dark Grey	Mudstone	Slight effervescences, organic matter halos. Angular blocky beds.	

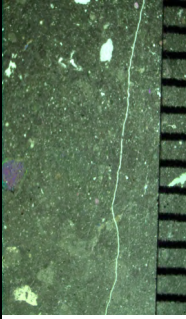
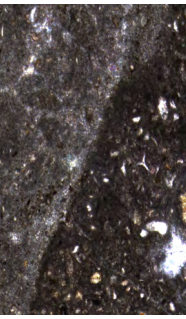

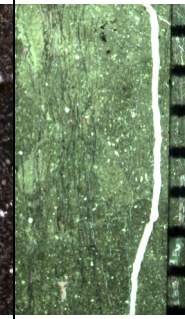
Sample #	Depth bed(m)	Depth total(m)	Color	Lithology	Description	Notes/Thin Section Image
KU-PR3-13	0.52	40.91	Grey → Purple	Mudstone	Some 0.1-1cm carbonate nodules, slightly effervescent matrix. Not as dark grey as overlying unit. Angular blocky peds.	
KU-PR3-14	0.5	40.39	Purple → Grey	Mudstone	Root traces with halos, gradation change from this unit in to greyer overlying unit. Some 2-5cm diameters carbonate nodules. Matrix mudstone is very effervescent.	
KU-PR3-15A/B	0.71	39.89	Purple → Grey	Carbonate nodule bearing mudstone	Effervescent matrix(A), with 20cm diameter nodules.(B)	A.  B. 

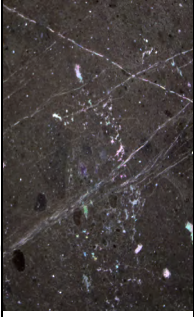
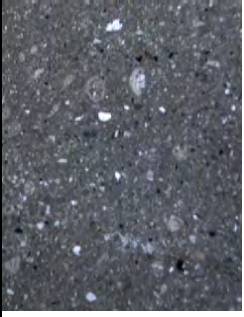
Sample #	Depth bed(m)	Depth total(m)	Color	Lithology	Description	Notes/Thin Section Image
KU-PR3-16A/B	0.63	39.18	Purple	Carbonate nodule bearing mudstone	Large 5-20cm diameters carbonate nodules. Slight effervescences in mudstone matrix, Some organic matter halos. Angular blocky peds.	
KU-PR3-17	0.68	38.55	Grey → Purple	Mudstone	Very friable, slight effervescences, angular blocky peds. Image is cross polarized.	
KU-PR3-18	0.68	37.87	Grey	Mudstone	No effervescence, angular blocky peds.	
KU-PR3-19	0.48	37.19	Grey	Mudstone	Ref. PR3-18	
KU-PR3-20	0.62	36.71	Grey	Mudstone	Matrix has slight effervescences some carbonate nodules, 1-3cm in diameter, sub-angular blocky peds.	
KU-PR3-21A/B	0.48	36.09	Grey	Mudstone	Matrix is very friable and not effervescent; with some carbonate nodules 0.1-4cm in diameter. Peds are sub-angular blocky.	

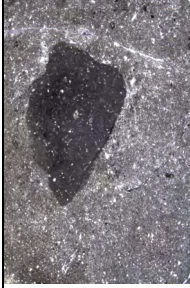
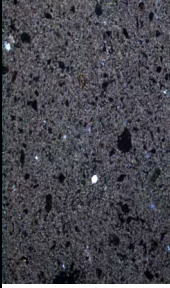


Sample #	Depth bed(m)	Depth total(m)	Color	Lithology	Description	Notes/Thin Section Image
KU-PR3-22A/B	0.49	35.61	Grey	Indurated Carbonate	Carbonate bed (A) is cemented in place, surrounding mudstone(B) has no effervescences. Forms a small slope break.	A.  B. 
KU-PR3-23A/B	0.58	35.12	Grey	Mudstone	Some small carbonate nodules 0.1-1cm in diameter (A). Many modern roots through this unit.	A. 
KU-PR3-24	0.45	34.54	Grey → Brown	Mudstone	Gradational transition from grey to brown color through the unit. No effervescences in matrix but some small 0.1-1cm carbonate nodules occur along planes. Peds are sub-angular blocky and very friable.	
KU-PR3-25	0.58	34.09	Grey → Red	Mudstone	Ref. PR3-24	


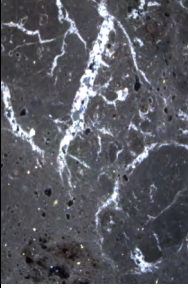
Sample #	Depth bed(m)	Depth total(m)	Color	Lithology	Description	Notes/Thin Section Image
KU-PR3-26	0.53	33.51	Grey→Red	Mudstone	No effervescence no carbonate nodules. Sub-angular blocky peds.	
KU-PR3-27	0.71	32.98	Grey	Mudstone	No effervescence in matrix, but some small 0.1-1cm diameter carbonates nodules (A). Image is cross polarized	A. 
KU-PR3-28A/B	0.66	32.27	Grey	Carbonate nodule bearing mudstone	No effervescence in matrix, Top 20cm of unit is a thin carbonate bed, with 10cm of small carbonate nodules 0.1-1cm diameter below this. Sub-angular blocky peds.	
KU-PR3-29	0.52	31.61	Grey	Mudstone	Matrix has no effervescence but unit contains carbonate nodules. Sub-angular blocky peds.	
KU-PR3-30	0.52	31.09	Grey	Mudstone	Carbonate nodules disappear, unit is not effervescent, no bedding, sub-angular blocky peds.	
KU-PR3-31	0.53	30.57	Grey	Mudstone	Effervescences, organic matter halos, very friable, sub angular blocky peds.	
KU-PR3-32	0.69	30.04	Grey	Mudstone	Very little/No effervescences. More clay enriched than overlying units.	

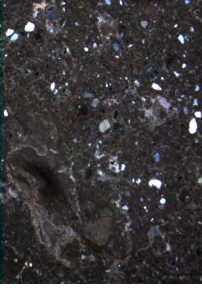
Sample #	Depth bed(m)	Depth total(m)	Color	Lithology	Description	Notes/Thin Section Image
KU-PR3-33	0.56	29.35	Grey/ Purple	Mudstone	Transitional boundary between purple and grey. No effervescences.	
KU-PR3-34	0.57	28.79	Purple→ Grey	Mudstone	No effervescences, sub-angular blocky peds.	
KU-PR3-35	0.57	28.22	Purple→ Grey	Mudstone	Purple coloration occurs as mottles, no effervescences, and sub-angular blocky peds.	
KU-PR3-36	0.86	27.65	Purple→ Grey	Mudstone	Oxidized plant root, purple halo. No effervescences, sub-angular blocky.	
KU-PR3-37	0.64	26.79	Grey→ Purple	Mudstone	Similar to overlying unit (Ref. PR3-36) oxidized organic matter halos', sub-angular blocky ped's with no effervescences,	
KU-PR3-38	0.43	26.15	Grey	Silty Mudstone	Rip-up like grey clay clasts'. More Silt sized grains than in overlying units. Abrupt upper boundary with overlying purple unit.	
KU-PR3-39	0.87	25.72	Grey	Silty Mudstone	Ref. PR3-40, but organic matter oxidation halos.	
KU-PR3-40	1.09	24.85	Grey	Silty Mudstone	No effervescences, very friable, SBK. Oxidized organic matter halos occur on inner faces of sub-angular blocky peds.	
KU-PR3-41	0.54	23.76	Dark Grey →Purple	Silty Mudstone	No effervescences; no obvious bedding. Abrupt contact with overlying lighter grey unit	

Sample #	Depth bed(m)	Depth total(m)	Color	Lithology	Description	Notes/Thin Section Image
KU-PR3-42	0.7	23.22	Purple/Red →Grey	Silty Mudstone	Gradational change to dark grey, less purple unit, no effervescences, very friable Ref. PR3-43	
KU-PR3-43	0.43	22.52	Purple/Red →Grey	Silty Mudstone		
Cover	1.27	22.09	Cover	Cover		
KU-PR4-22	0.26	20.82	Red/Orange e→Yellow	Carbonate cemented mudstone	Ledge forming top unit. Ref. PR4-17 for unit description.	
KU-PR4-21	0.5	20.56	Red/Orange e→Yellow	Carbonate cemented mudstone	Ref. PR4-17	
KU-PR4-20	0.94	20.06	Red/Orange e→Yellow	Carbonate cemented mudstone	Ref. PR4-17	
KU-PR4-19	0.94	19.12	Red/Orange e→Yellow	Carbonate cemented mudstone	Ref. PR4-17	

Sample #	Depth bed(m)	Depth total(m)	Color	Lithology	Description	Notes/Thin Section Image
KU-PR4-18	0.73	18.18	Red/Orange e→Yellow	Carbonate cemented mudstone	Ref. PR4-17	
KU-PR4-17	0.75	17.45	Red/Orange e→Yellow	Carbonate cemented mudstone	Carbonate cemented mudstone. Occurs in stacked beds, which stair-step upward. Thin-cemented beds occur between major beds, sampled at major beds. Very contorted nodular looking. Violently effervescent.	
KU-PR4-16	0.34	16.7	Purple/Red →Orange	Mudstone	Lithologically very similar to PR4-14, no beds, but coloration is lighter as this unit grades in to a more carbonate rich unit. No effervescences	
KU-PR4-15	0.53	16.36	Purple/Red	Mudstone	Ref. PR4-14	
KU-PR4-14	0.49	15.83	Purple/Red	Mudstone	No bedding planes, no effervescences.	

Sample #	Depth bed(m)	Depth total(m)	Color	Lithology	Description	Notes/Thin Section Image
Cover	3.96	15.34	Cover	Cover		
KU-PR4-13	0.3	11.38	Grey/Green	Carbonate nodule bearing mudstone	Ref. PR4-8	
KU-PR4-12	0.46	11.08	Grey/Green	Carbonate nodule bearing mudstone	Ref. PR4-8	
KU-PR4-11	0.4	10.62	Grey/Green	Carbonate nodule bearing mudstone	Ref. PR4-8. Image is cross polarized.	
KU-PR4-10	0.5	10.22	Grey/Green	Carbonate nodule bearing mudstone	Ref. PR4-8	
KU-PR4-9	0.36	9.72	Grey/Green	Carbonate nodule bearing mudstone	Ref. PR4-8	
KU-PR4-8	0.2	9.36	Grey/Green →Purple	Carbonate nodule bearing mudstone	Gradational coloration in bed, base is grey grades in to purple unit at the top. Very effervescent. Carbonate nodules occur in lenticular beds, pinch out. Image was cross polarized.	

Sample #	Depth bed(m)	Depth total(m)	Color	Lithology	Description	Notes/Thin Section Image
Cover	2.62	9.16	Cover	Cover		
KU-PR4-7	2.7	6.54	White/Pink	Sandstone	Very fine-lower medium sandstone. Effervescent.	
KU-PR4-6	1.06	3.84	White/Pink	Sandstone	Fining upward, cross-laminated, paleocurrent direction is SE. Upper fine-Medium sandstone. Effervescent.	
KU-PR4-5	0.2	2.78	White/Pink	Sandstone	Few basal carbonate nodules that have been coated with sandstone. Infilling of sandstone unit. Erosive but could not erode the carbonate nodules. Coarse material at base, fining upward unit. Medium-Coarse sandstone. Effervescent.	
KU-PR4-4	0.35	2.58	Purple	Mudstone	Few carbonate nodules in this unit, lenticular in shape, infilling above the underlying carbonate unit, which forms a depression on the top.	
KU-PR4-3	0.54	2.23	Grey/Purple	Indurated Carbonate	Stacked indurated carbonated unit, voids between large nodules filled with grey/purple mudstone.	

Sample #	Depth bed(m)	Depth total(m)	Color	Lithology	Description	Notes/Thin Section Image
KU-PR4-2	0.77	1.69	Grey	Carbonate nodule bearing mudstone	No purple mottling, more carbonate nodules than underlying unit, grades into overlying indurated carbonate bed.	
KU-PR4-1	0.92	0 → 0.92	Grey → Purple	Carbonate nodule bearing mudstone	No effervescences in mudstone, purple is mottled with grey, horizontal-bedding planes. Some carbonate nodules.	

Appendix D: Stable Isotope Data for KU-Price River 1 Section

Distance Above Base (m)	Sample #	$\delta^{13}\text{C}_{\text{org}}$ VPDB	TOC (%)
18.79	KU-PR1-50	-16.70	0.19
18.79	KU-PR1-50- Replicate	-16.36	0.30
20.07	KU-PR1-47	-14.01	0.67
20.71	KU-PR1-46	-13.23	0.64
21.78	KU-PR1-45	-14.08	0.56
22.02	KU-PR1-44	-15.67	0.23
23.28	KU-PR1-41	-18.24	0.35
23.78	KU-PR1-40	-15.15	0.75
24.28	KU-PR1-39	-15.06	0.83
24.78	KU-PR1-38	-19.45	1.61
25.28	KU-PR1-37	-19.06	0.96
25.78	KU-PR1-36	-19.47	0.61
26.28	KU-PR1-35	-15.02	0.85
27.14	KU-PR1-34	-15.26	0.37
27.39	KU-PR1-33	-13.03	0.58
27.64	KU-PR1-32	-13.15	0.69
28.54	KUPR1-31	-14.93	0.64
29.12	KU-PR1-30	-16.55	0.27
29.37	KU-PR1-29	-16.03	0.30
29.84	KU-PR1-28	-14.95	0.67
30.11	KU-PR1-27	-14.49	0.77
30.38	KU-PR1-26	-14.55	0.67
30.73	KU-PR1-25	-13.62	0.80
31	KU-PR1-24	-7.77	1.39
32.68	KU-PR1-22	-12.82	1.03
32.95	KU-PR1-21	-15.75	0.23
33.33	KU-PR1-20	-15.49	0.34
33.33	KU-PR1-20- Replicate	-14.49	0.72
34.06	KU-PR1-19	-16.35	0.64
34.42	KU-PR1-18	-14.56	0.76
36.78	KU-PR1-16- Replicate	-14.56	0.89

Distance Above Base (m)	Sample #	$\delta^{13}\text{C}_{\text{org}}$ VPDB	TOC (%)
38.29	KU-PR1-15	-14.03	0.85
40.24	KU-PR1-14	-14.98	0.98
41.56	KU-PR1-13	-15.03	1.11
43.41	KU-PR1-12	-15.19	0.26
44.82	KU-PR1-11	-15.03	0.27
55.1	KU-PR1-4	-14.06	0.34

Appendix E: Stable Isotope Data for KU Price River-2 Section

Distance Above Base (m)	Sample #	$\delta^{13}\text{C}_{\text{org}}$ VPDB	TOC (%)
0.96	KU-PR2-37	-20.06	0.09
1.46	KU-PR2-36	-17.28	0.04
6.52	KU-PR2-32	-16.94	0.20
10.12	KU-PR2-30A	-15.90	0.10
10.12	KU-PR2-30B	-22.19	0.27
13.9	KU-PR2-29	-17.56	0.15
15.1	KU-PR2-28A	-18.23	0.28
15.6	KU-PR2-28B	-17.87	0.18
17.1	KU-PR2-28C	-19.18	0.20
20.6	KU-PR2-27	-16.58	0.20
21.1	KU-PR2-26	-17.46	0.15
22.77	KU-PR2-24A	-18.25	0.23
22.77	KU-PR2-24B	-22.27	0.06
23.74	KU-PR2-23A	-18.13	0.27
23.74	KU-PR2-23B	-18.95	0.25
24.5	KU-PR2-22	-17.13	0.11
26.05	KU-PR2-21	-17.21	0.07
27.12	KU-PR2-20	-16.67	0.17
29.4	KU-PR2-19	-18.58	0.26
30.66	KU-PR2-17	-17.98	0.10
31.45	KU-PR2-16	-18.08	0.06
33.74	KU-PR2-14	-20.66	0.08
35.07	KU-PR2-13	-19.33	0.06
35.24	KU-PR2-12	-13.80	0.07
35.73	KU-PR2-11	-18.26	0.34
36.39	KU-PR2-10	-17.27	0.13
36.93	KU-PR2-9	-18.87	0.18
36.93	KU-PR2-9-Replicate	-18.63	0.31
37.3	KU-PR2-8	-16.51	0.15
37.7	KU-PR2-7	-16.45	0.21
39.67	KU-PR2-5	-17.83	0.20
39.67	KU-PR2-5-Replicate	-17.63	0.28
39.97	KU-PR2-4	-17.89	0.23
40.45	KU-PR2-3	-17.87	0.31
40.95	KU-PR2-2	-16.38	0.42

Appendix F: Stable Isotope Data for KU-Price River 3/4 Section

Distance Above Base (m)	Sample #	$\delta^{13}\text{C}_{\text{org}}$ VPDB	TOC (%)
2.23	KU-PR4-3B	-15.14	0.25
2.58	KU-PR4-4	-15.97	0.13
9.72	KU-PR4-9B	-14.92	0.51
10.62	KU-PR4-11B	-13.52	0.40
11.08	KU-PR4-12B	-16.38	0.16
15.83	KU-PR4-14	-15.59	0.20
16.36	KU-PR4-15	-15.76	0.16
16.7	KU-PR4-16	-15.99	0.16
20.82	KU-PR4-22	-15.43	0.18
23.22	KU-PR3-42	-17.08	0.06
23.76	KU-PR3-41	-15.52	0.26
24.85	KU-PR3-40	-16.67	0.05
25.72	KU-PR3-39	-13.37	0.16
26.15	KU-PR3-38	-16.93	0.08
26.79	KU-PR3-37	-16.17	0.08
27.65	KU-PR3-36	-17.15	0.08
28.22	KU-PR3-35	-16.79	0.07
28.79	KU-PR3-34	-17.96	0.08
29.35	KU-PR3-33A	-16.05	0.07
29.35	KU-PR3-33B	-15.62	0.06
30.04	KU-PR3-32	-20.38	0.08
31.09	KU-PR3-30	-17.18	0.08
31.61	KU-PR3-29A	-17.23	0.09
32.98	KU-PR3-27A	-19.68	0.06
33.51	KU-PR3-26	-15.42	0.33
34.09	KU-PR3-25	-15.85	0.10
34.54	KU-PR3-24	-17.03	0.10
35.12	KU-PR3-23A	-16.65	0.12
35.61	KU-PR3-22B	-17.67	0.08
36.09	KU-PR3-21B	-17.43	0.14
37.87	KU-PR3-18	-14.12	0.17
39.89	KU-PR3-15A	-14.41	0.14
40.39	KU-PR3-14B	-14.42	0.14

Distance Above Base (m)	Sample #	$\delta^{13}\text{C}_{\text{org}}$ VPDB	TOC (%)
41.45	KU-PR3-12A	-20.14	0.39
42.05	KU-PR3-11	-18.42	0.30
42.63	KU-PR3-10B	-17.99	0.25
43.35	KU-PR3-9A	-17.88	0.40
44.61	KU-PR3-7	-12.84	0.90
45.27	KU-PR3-6	-16.25	0.20
46.18	KU-PR3-5	-15.68	1.00
49.35	KU-PR3-1	-24.80	0.14

Appendix G: KU-Muddy Creek Section, Goblin State Park Utah.

For detailed site location, information including longitude and latitude of sites or to visit site locations in this study, please contact the State Paleontologist, Utah Geological Survey, 1594 West North Temple, Suite 3110, P.O. Box 146100 Salt Lake City, UT 84114-6100; TEL (801) 537-3307 FAX (801) 537-3400

Sample #	Depth bed (m)	Depth total (m)	Color Dominant color → sub-color	Lithology	Description	Notes
KU-MC-33	0.75	16.25	Purple/Green mottled	Mudstone	Clay cutans and some small slickensides.	
KU-MC-32	0.5	15.75	Purple/Green mottled	Mudstone	Some slickensides	
KU-MC-31	0.75	15.25	Purple/Green mottled	Mudstone	Slickensides with some orange oxidatized surfaces	
KU-MC-30	0.25	14.50	Darker grey → green	Mudstone	Very friable, with orange oxidized coatings on surfaces	
KU-MC-29	0.75	14.25	Darker grey → green	Mudstone	Very friable, with orange oxidized coatings on surfaces	
KU-MC-28	0.25	13.5	Grey → Orange mottles	Mudstone	Same as MC-27	
KU-MC-27	0.75	13.25	Grey → Orange mottles	Mudstone	Fine grained, massive mudstone with mottling.	
KU-MC-26	0.75	12.50	Purple/Green grey	Mudstone	Purple and Green are mottled, massive, similar to underlying mudstone	
KU-MC-25	0.25	11.75	Grey with Green/Red mottling	Mudstone	Lithologically same as MC-24 but with more mottling.	

Sample #	Depth bed (m)	Depth total (m)	Color Dominant color → sub-color	Lithology	Description	Notes
KU-MC-24	0.25	11.25	Green/Red mottled	Silty mudstone	Some secondary oxidation, ped's are subangular blocky to angular blocky	
KU-MC-23	0.25	10.75	Purple/Green mottled	Silty mudstone	Massive, gradational boundary between underlying sandstone and silty mudstone. Clasts are angular or sub angular blocky.	
KU-MC-22	0.5	10	White/light tan with Purple/green clasts	Sandstone	Very fine-grained sandstone with some variegated colored clasts.	
KU-MC-21	0.5	9.5	White/light tan	Sandstone	Same as MC-20	
KU-MC-20	0.25	9.00	White/light tan	Sandstone	Fine sand with no bioclasts.	
KU-MC-19	0.5	8.5	White/light tan	Sandstone	Fine sandstone, with dark <1cm clasts, and some snail bioclasts.	
KU-MC-18	0.25	8.0	White/Purple mottled	Wackestone	Sandy mudstone, no bioclasts.	
KU-MC-17	0.25	7.75	White/Purple mottled	Sandstone	Same as MC 15 and 16	

Sample #	Depth bed (m)	Depth total (m)	Color Dominant color → sub-color	Lithology	Description	Notes
KU-MC-16	0.25	7.5	White/light tan	Sandstone	Fine to medium sandstone, some organic matter (plant detritus) otherwise similar to MC-15.	
KU-MC-15	0.25	7.25	White/light tan	Sandstone	Fine to medium sandstone with Snail carapaces, fish bones and scales, abrupt contact with MC-14. Snail carapaces occur in multiple beds.	
KU-MC-14	0.25	7	Purple/Green	Reworked tuff	Abrupt contact with MC-13, very glassy looking, high biotite lenses.	
KU-MC-13	0.25	6.75	White/Pink	Very fine sand	Same as MC-12	
KU-MC-12	0.25	6.5	White/Pink	Very fine sand	Sandstone is indurated, but there are some very small (<2mm) lithics.	
KU-MC-11	0.25	6.25	Green	Very fine sand	Very fine sand, abrupt contact with top of MC-10.	
KU-MC-9	0.5	5.5	Green/light grey	Sandstone	Same as MC-8 but with more clayey lithics.	

Sample #	Depth bed (m)	Depth total (m)	Color Dominant color → sub-color	Lithology	Description	Notes
KU-MC-8	0.5	5	Grey/light green	Sandstone	Medium to fine sandstone with biotite flecks, some small clay lithic fragments (1-5 mm) but generally well sorted. Weathers out and appears laminated.	
KU-MC-7	0.5	4.5	Variegated Color	Conglomerate	Fining upward to sandstone, from a cobble lag. Cobbles are in a sandy matrix	
KU-MC-6	0.25	4.25	Green/white	Laminated clayey-sandstone	Green, clay rich material then white very fine sandstone	
KU-MC-5	0.25	4	Green/white (layered)	Laminated clayey-sandstone	White is fine grained sandstone (Quartz rich), Green material is clay rich.	
KU-MC-4	0.75	3.75	Dark green	Claystone	Gradual change from sandstone below to very fine grained clayey mudstone.	
KU-MC-2	1	2	Green/light green	Fine grained sandstone	Massively bedded, well sorted.	

Sample #	Depth bed (m)	Depth total (m)	Color Dominant color → sub-color	Lithology	Description	Notes
KU-MC-1	0.5	1.5	Green → yellow	Fine grained sandstone	Massively bedded, well sorted. Fine grained	
KU-MC-0	1	1	Tan-brown	Sandstone		

Appendix H: Geochronology and stable isotope data KU- Muddy Creek Section

The KU-Muddy Creek Section, KU-MC was measured and sampled in the summer of 2006. The stratigraphic section was measured and described along trenched surfaces. Oriented samples were collected at 0.5 m to 0.25m. Samples were also collected at boundaries where any lithologic or significant color change occurred. At these intervals, color, lithology, sedimentary structures as well as the presence of any fossils or trace fossils were noted.

The section measures approximately 20m, a fluvially reworked ash, with high biotite content was sampled, for detrital zircon dating, at the University of Kansas Isotope Geochemistry Lab, under the supervision of D.F. Stockli. While sedimentary rocks were collected above and below this ash for $\delta^{13}\text{C}_{\text{org}}$ analysis at the University of Kansas W. M. Keck Paleoenvironmental and Environmental Stable Isotope Laboratory under the direction of L. Gonzalez.

Samples were double dated to measure both (U-TH)/He and U/Pb ages on the same detrital zircon crystal. Double dating was conducted to help characterize the frequency distribution of populations of crystals with distinct combinations of ages in the rock. Approximately 25 single zircon crystals were hand picked, from mineral separates, based on crystal size and shape (euhedral crystal, 60-140 μm width and 150-100 μm length). All crystals were digitally photographed and measured for alpha-ejection corrections.

Two different analytical techniques were then used to obtain a combined (U-Th)/He and U/Pb age on a single grain. Techniques similar to those modified from Krogh (1973,1982) Rahl et al (2003) and Reiners et al. (2005) were used to prepare and analyze samples.

$\delta^{13}\text{C}_{\text{org}}$ For Muddy Creek Section (KU-MC)

Depth from base(m)	Sample #	d13C VPDB	C%
1.5	KU-MC-1	-14.17	0.06
2	KU-MC-2	-7.71	0.07
3	KU-MC-3	-14.96	0.05
3.75	KU-MC-4	-12.74	0.13
4.25	KU-MC-6	-11.24	0.07
5.5	KU-MC-9	-10.85	0.09
6	KU-MC-10	-14.91	0.05
6.25	KU-MC-11	-10.81	0.08
6.5	KU-MC-12	-17.68	0.07
6.75	KU-MC-13	-11.76	0.43
7	KU-MC-14	-15.53	0.28
7.5	KU-MC-16	-8.28	0.11
7.75	KU-MC-17	-8.82	0.18
8	KU-MC-18	-12.93	0.12
8.5	KU-MC-19	-8.79	0.17
9	KU-MC-20	-15.67	0.31
9.5	KU-MC-21	-7.07	0.15
10	KU-MC-22	-13.85	0.11
10.75	KU-MC-23	-10.13	0.11
11.25	KU-MC-24	-12.82	0.08
11.75	KU-MC-25	-15.31	0.33
12.5	KU-MC-26	-9.67	0.24
13.25	KU-MC-27	-14.26	0.08
13.5	KU-MC-28	-10.61	0.15
14.25	KU-MC-29	-8.72	0.46
14.5	KU-MC-30	-15.00	0.31
14.5	KU-MC-31	-9.63	0.14
15.25	KU-MC-31	-9.73	0.20
15.75	KU-MC-32	-13.40	0.09
16.25	KU-MC-33	-9.92	0.19

Figure 1H . Muddy Creek stratigraphic section with location of fluvially reworked ash bed indicated by the red star. Figure also shows TOC and $\delta^{13}\text{C}_{\text{org}}$ chemostratigraphy.

